

พลังงานสถานะพื้นของโลหะไฮโดรเจนสถานะของแข็งโดยวิธีวิกเนอร์ไฮท์ซและAPW



นายไพโรจน์ มุลตระกูล

วิทยานิพนธ์นี้เป็นส่วนหนึ่งของการศึกษาตามหลักสูตรปริญญาวิทยาศาสตรมหาบัณฑิต

สาขาวิชาฟิสิกส์ ภาควิชาฟิสิกส์

คณะวิทยาศาสตร์ จุฬาลงกรณ์มหาวิทยาลัย

ปีการศึกษา 2546

ISBN 974-17-3660-6

ลิขสิทธิ์ของจุฬาลงกรณ์มหาวิทยาลัย

GROUND STATE ENERGY OF SOLID METALLIC HYDROGEN BY THE
WIGNER-SEITZ METHOD AND APW



Mr. Pairot Moontragoon

A Thesis Submitted in Partial Fulfillment of the Requirements
for the Degree of Master of Science in Physics

Department of Physics
Faculty of Science

Chulalongkorn University

Academic Year 2003

ISBN 974-17-3660-6

Thesis Title Ground State Energy of Solid Metallic Hydrogen by the Wigner-
Seitz Method and APW

By Pairot Moontragoon

Field of Study Physics

Thesis Advisor Assistant Professor Udomsilp Pinsook

Accepted by the Faculty of Science, Chulalongkorn University in Partial
Fulfillment of the Requirements for the Master 's Degree

..... Dean of Faculty of Science
(Associate Professor Wanchai Phothiphichitr, Ph.D.)

THESIS COMMITTEE

..... Chairman
(Associate Professor Wichit Sritrakool, Ph.D.)

..... Thesis Advisor
(Assistant Professor Udomsilp Pinsook, Ph.D.)

..... Member
(Burin Asavapibhop, Ph.D.)

..... Member
(Somrit Wongmaneerod, Ph.D.)

ไพโรจน์ มูลตระกูล : พลังงานสถานะพื้นของโลหะไฮโดรเจนสถานะของแข็งโดยวิธีวิกเนอร์-ไซท์ซ์และAPW. (GROUND STATE ENERGY OF SOLID METALLIC HYDROGEN BY THE WIGNER-SEITZ METHOD AND APW) อ. ที่ปรึกษา : ผศ. ดร.อุดมศิลป์ ปิ่นสุข, 82หน้า. ISBN 974-17-3660-6.

เราได้คำนวณพลังงานสถานะพื้นของโลหะไฮโดรเจนสถานะของแข็งซึ่งเป็นฟังก์ชันของ r_s โดยใช้วิธีวิกเนอร์-ไซท์ซ์และวิธีคลื่นระนาบที่ขยายแบบเชิงเส้นในพลังงานศักย์เต็มรูป และระบุค่า r_s ที่พลังงานสถานะพื้นที่มีค่าต่ำสุดภายใต้พลังงานศักย์แบบคูลอมบ์และพลังงานศักย์ก้างแบบกระจายสม่ำเสมอและแบบโรมัส-เฟร์มี ในวิธีของของวิกเนอร์-ไซท์ซ์เราได้ประมาณการกระจายของแถบพลังงานให้ละเอียดถึงอันดับ k^4 และใช้พลังงานสหสัมพันธ์ที่ยอมรับที่สุดเท่าที่จะหาได้ เพื่อคำนวณโดยวิธีวิกเนอร์-ไซท์ซ์ให้ละเอียดขึ้นเราได้ใช้วิธีคลื่นระนาบที่ขยายแบบเชิงเส้นในพลังงานศักย์เต็มรูปเพื่อคำนวณพลังงานสถานะพื้น ความหนาแน่นสถานะ และโครงสร้างแถบพลังงาน ในโครงผลึกหลายๆแบบ เราได้พบว่าสำหรับโครงผลึกที่มีสมมาตรมากๆ วิธีทั้งสองให้ผลใกล้เคียงกัน และไฮโดรเจนสถานะของแข็งภายใต้แบบจำลองของเราจะเป็นโลหะ

สถาบันวิทยบริการ
จุฬาลงกรณ์มหาวิทยาลัย

ภาควิชาฟิสิกส์
สาขาวิชาฟิสิกส์
ปีการศึกษา 2546

ลายมือชื่อนิสิตร.....
ลายมือชื่ออาจารย์ที่ปรึกษา.....

4372360123 : MAJOR PHYSICS

KEY WORD: METALLIC HYDROGEN / WIGNER-SEITZ METHOD / FULL POTENTIAL LINEARIZED AUGMENTED PLANE WAVE / HARTREE-FOCK THEORY / DENSITY FUNCTIONAL THEORY

PAIROT MOONTRAGOON : GROUND STATE ENERGY OF SOLID METALLIC HYDROGEN BY THE WIGNER-SEITZ METHOD AND APW.
THESIS ADVISOR : ASST. PROF. DR. UDOMSILP PINSOOK, 82 pp. ISBN 974-17-3660-6.

We calculate the ground state energy of solid metallic hydrogen as a function of r_s , using the Wigner-Seitz method and full potential linearized augmented plane wave (FP-LAPW), and to determine r_s at which the ground state energy is minimum. The Coulomb, uniform screened Coulomb and Thomas-Fermi screened Coulomb potentials are used in the Wigner-Seitz calculation. We estimate the energy dispersion up to $O(k^4)$ and use the most acceptable correlation energy. To refine the Wigner-Seitz method, we employ the FP-LAPW to determine the ground state energy and the density of states as well as the band structures in various lattice structures. We find that, for a high symmetry lattice, both methods give similar results and solid hydrogen in our model is a metal.



Department Physics

Field of study Physics

Academic year 2003

Student's signature.....

Advisor's signature.....

ACKNOWLEDGEMENTS

I would like to dedicate this section to give my special gratitude to the people who help and support me through my master thesis work. Without anyone of them, it would be impossible for this thesis to be finished.

First of all I would like to express my great thanks to my advisor, Assistant Professor Dr. Udomsilp Pinsook. This thesis work has gone through a lot of problems and difficult time, but he has a great patient and gives suggestions which help me to solve all these problems. I am also grateful to the fathering people:

Mr. Saran Phibanchon for giving me a book of Many Body Theory.

All my friends which include Mr. Pornjuk Sripusharawoot, Mr. Aphirat Phusittrakool, and others, who made the life very pleasant and interesting experience for me.

I would like to thank my family who always believe in me and support me in every way they can.

Finally, my sincere thanks to the Development and Promotion of Science and Technology talents project of Thailand (DPST) for supporting fund.

สถาบันวิทยบริการ
จุฬาลงกรณ์มหาวิทยาลัย

CONTENTS

vii

	Page
THAI ABSTRACT	iv
ENGLISH ABSTRACT.....	v
ACKNOWLEDGEMENT	vi
CONTENTS.....	vii
LIST OF FIGURES	x
CHAPTER 1	1
INTRODUCTION.....	1
1.1 Introduction.....	1
1.2 Objectives	2
1.3 Thesis Outline	3
CHAPTER 2	5
THE MANY ELECTRON THEORY	5
2.1 Introduction.....	5
2.1.1 Born-Oppenheimer Approximation.....	6
2.1.2 One Electron Approximation.....	7
2.2 Hartree Approximation	7
2.3 Hartree-Fock Approximation.....	9
2.4 Density Functional Approximation.....	11
2.4.1 Local Density Approximation (LDA).....	14
CHAPTER 3	16
THE WIGNER-SEITZ METHOD	16
3.1 Introduction.....	16
3.2 The Cellular Method.....	17
3.3 Model Potentials.....	22
3.3.1 Coulomb Potential	22
3.3.2 Screening Effects	23
3.4 Hartree Energy.....	27
3.5 Exchange Energy	28
3.6 Correlation Energy	28

CONTENTS (Cont.)

viii

	Page
CHAPTER 4	31
THE FULL POTENTIAL LINEARIZED AUGMENTED PLANE WAVE	31
4.1 Introduction.....	31
4.2 The Augmented Plane Wave (APW).....	33
4.3 The Linearized Augmented Plane Wave (LAPW)	39
4.4 Brillouin Zone Integration.....	44
4.4.1 The Body-Centered Cubic Lattice	45
4.4.2 The Face-Centered Cubic Lattice	46
4.4.3 The Hexagonal Close-Packed Lattice.....	47
4.4.4 The Tetrahedron Method	50
4.5 The Full Potential Linearized Augmented Plane Wave (FP-LAPW).....	55
4.5.1 Construction of the Full Potential	57
4.5.2 Construction of the Full Hamiltonian	60
4.5.3 Mixing Scheme	61
4.5.4 Total Energy Calculation	62
CHAPTER 5	64
CALCULATION OF THE GROUND STATE ENERGY	64
5.1 Introduction.....	64
5.2 The Total Ground State Energy of Solid Metallic Hydrogen by the Wigner- Sietz Method	64
5.3 The Ground State Properties of the Solid Metallic Hydrogen by the Full Potential Linearized Augmented Plane Wave Method.....	66
5.3.1 The Energy Band Structure.....	67
5.3.2 The Density of States.....	68
5.3.3 The total Ground State Energy	70
5.4 Discussion.....	72
CHAPTER 6	76
CONCLUSIONS	76
REFERENCES	79
BIOGRAPHY	82

List of Figures

ix

	Page
Figure 2.1: A self-consistent method, which is used in the density functional theory.	14
Figure 3.1: Atomic polyhedral for (a) the body-centered cubic lattice, (b) the face-centered cubic lattice, (c) the hexagonal close-packed lattice	17
Figure 4.1: The muffin tin potential approximation used in the augmented plane waves. \vec{r}_v is a position of each atom, \vec{r} is a local coordinate in the sphere, centered at the atom position, and $\vec{\rho}$ is a position vector which relative to origin and can be expressed as $\vec{\rho} = \vec{r}_v + \vec{r}$	34
Figure 4.2: The APW determinant of $H_{pq} + S_{pq} - EO_{pq}$ must be evaluated for number of energies E. The square indicates the eigenenergies of the valence electrons in face-centered cubic copper at $\vec{k} = \frac{2\pi}{a}(0.74, 0.74, 0.74)$ and $a=6.8222a_0$	38
Figure 4.3: Parts of the radial l composition of a LAPW basis function for Cesium for the same \vec{k} point	41
Figure 4.4: The fundamental domain of \vec{k} or first Brillouin zone for (a) the body-centered cubic lattice (b) the face-centered cubic lattice and (c) the hexagonal close-packed lattice	49
Figure 4.5: Break up of a sub mesh cell into six tetrahedra.....	51
Figure 5.1: Ground state energy calculated by the Wigner-Seitz method with various potential: the Coulomb potential (solid line), the uniform screened potential (long dashed line), the Thomas-Fermi screened potential (short dashed line)	65
Figure 5.2: The energy band structure of the solid metallic hydrogen in face-centered cubic structure	67
Figure 5.3: The energy band structure of the solid metallic hydrogen in body-centered cubic structure	67
Figure 5.4: The energy band structure of the solid metallic hydrogen in hexagonal close-packed structure.....	68
Figure 5.5: The density of states of the solid metallic hydrogen in a face-centered cubic structure	69
Figure 5.6: The density of states of the solid metallic hydrogen	

List of Figures (Cont.)

x

	Page
in a body-centered cubic structure	69
Figure 5.7: The density of states of the solid metallic hydrogen in a hexagonal close-packed structure	70
Figure 5.8: The total ground state energy of metallic hydrogen with various atomic structure: a face-centered cubic (long dashed line), body-centered cubic (solid line) and hexagonal close packed (short dashed line)	71
Figure 5.9: A comparison of the total ground state energy of metallic hydrogen between Wigner-Seitz method and the full potential linearized augmented plane wave	74



สถาบันวิทยบริการ
จุฬาลงกรณ์มหาวิทยาลัย

Chapter 1

Introduction

1.1 Introduction

Hydrogen is the lightest element in the periodic table. In 1935, when quantum mechanics was firmly established, Wigner and Huntington[1] predicted that hydrogen could become a metal under enormously intense pressure. Since then it stimulated an enormous amount of works in the search for metallic hydrogen. This goal actually revealed much harder works than what initially expected. Wigner and Huntington predicted a metallization pressure of 25 GPa. It is shown experimentally that this estimation was too optimistic. So far, in 2003, metallization has not been observed in crystalline hydrogen at least up to the pressure of 340 GPa. The metallic hydrogen is of great scientific interests because it is definitely the lightest metal. Some calculations[2] indicated that it can be in a superconducting state even at high temperatures. A possible technological application is to use metallic hydrogen as a very compact source for fuel cells. Furthermore, some

evidences showed that the cores of Jupiter and Saturn are composed of metallic hydrogen[3]. In this work, we would like to understand more about solid metallic hydrogen. We assume that solid metallic hydrogen is a neutral collection of static protons, which occupy a high symmetry lattice, and electrons. The ground state energy of solid metallic hydrogen is calculated by using the Hartree-Fock approximation[4-5] or the density functional approximation[5-6]. Our primary goal is to determine the ground state energy of solid metallic hydrogen as function of r_s , and to determine r_s at which the ground state energy is minimum.

However, the determination of the phase transition point is very difficult. According to experiments, hydrogen does not become a metallic solid under the highest pressure available in laboratories, i.e. about 340 GPa. Furthermore, solid molecular hydrogen[7] has lower ground state energy which is -1.1648 Ry/atom at $r_s = 3.12a_0$. Thus it is more likely that solid molecular hydrogen will be found under high pressure instead of the solid metallic hydrogen because the nature will be in its lowest energy state. The solid metallic hydrogen might exist as a metastable state. This work aims to study whether stable or metastable metallic states.

1.2 Objectives

The purpose of this work is to calculate the ground state energy of solid metallic hydrogen as a function of r_s and to determine r_s at which the ground state energy

is minimum. We carry out two similar methods. In the first method, we use the Hartee-Fock approximation to solve a many-body problem of electrons moving in a potential field and use the Wigner-Seitz method to accurately estimate the energy band dispersion upto order of k^4 using the most accurate available correlation potential. Hence the ground state energy obtained in this work is more accurate than that of previous works[7]. However, the major weakness of this method is that the proper lattice symmetry is not taken into account.

Therefore, the ground state energy, the band structure and the density of states of solid metallic hydrogen in various lattice structures, such as body centered cubic, faced centered cubic and hexagonal close packed are also investigated by an alternative formalism. This is aimed to refine our calculations in order to include the effect of lattice structures. We choose the full potential linearized augmented plane wave (FP-LAPW) method which imposes the density functional theory to solve many-electron problems. The ground state energy depends on lattice structures and can be expressed as a function of lattice constants. From this relation, a stable lattice constant and a corresponding lattice structure, of which the ground state energy is minimum, are determined.

1.3 Thesis Outline

This thesis is organized as follows: chapter 1 provides an introduction to previous works and the possibility of their extension. The objectives of this work are

stated. In chapter 2, the Hartree-Fock approximation and the density functional are discussed in general. The many-electrons problem can be reduced to a one electron problem by using the Hartree-Fock approximation, the density functional approximation and some other approximations such as the Born-Oppenheimer approximation and the independent particle local density approximation. In chapter 3, we discuss a more specific method for calculating the ground state energy of solid metallic hydrogen by using the Hartree-Fock approximation. The energy dispersion is calculated by the Wigner-Seitz method. This dispersion depends on the density of the metal but does not depend on the information of lattice structures. In chapter 4, a more complicate theory, which can be used to calculate the ground state energy, the energy bands and the density of states of the the metal in various lattice structures, is presented. This method is an interplay between the density functional theory and the full potential linearized augmented plane wave method. In chapter 5, the results of calculations, such as the ground state energy, the energy band, and other properties in different lattice structures and different lattice constants are presented. This formation can be used for determining the possible macroscopic states of solid metallic hydrogen. Conclusions are in chapter 6.

Chapter 2

The Many Electron Theory

2.1 Introduction

In this chapter, the Hartree-Fock theory and the density functional theory, which are two different approaches to the many-electron problem, are discussed. Both theories are the simplification of the full problem of many-electrons moving in a potential field. A physical system consists not only of electrons but also of nuclei and each of these particles move in the field generated by the others. The Hamiltonian of the system consisting of N electrons and K nuclei is

$$H = \sum_{i=1}^N \frac{p_i^2}{2m} + \sum_{n=1}^K \frac{P_n^2}{2M_n} + \frac{1}{2} \sum_{i,j=1; i \neq j}^N \frac{e^2}{|\vec{r}_i - \vec{r}_j|} - \sum_{n=1}^K \sum_{i=1}^N \frac{e^2 Z_n}{|\vec{r}_i - \vec{R}_n|} + \frac{1}{2} \sum_{n,n'=1; n \neq n'}^K \frac{e^2 Z_n Z_{n'}}{|\vec{R}_n - \vec{R}_{n'}|}, \quad (2.1)$$

where the index i, j refer to the electrons and n, n' to the nuclei, e, r_i, p_i , and m are the charges, position, momentum and the mass of the electrons, Z_n, R_n, P_n and M_n are the charges, position, momentum and the mass of different nuclei. The first and second terms are the kinetic energies of electrons and nuclei respectively.

The third term is the coulomb repulsion between the electrons and the fourth term is the coulomb attraction between the electrons and the nuclei. The last term is the coulomb repulsive between the nuclei. It is impossible to solve the stationary Schrödinger equation for this Hamiltonian directly. In a few following subsections, we will introduce some approximations.

2.1.1 Born-Oppenheimer Approximation

In a system consisting of both heavy and light particles, we can assume, to a high degree of accuracy, that the movement of the heavy particles (ions) can not quite follow the dynamics of the light particles (electrons). The motions of the nuclei are slower than those of the electrons because the mass of a proton or a neutron is about 1835 times larger than the electron mass. Thus we may separate the degree of freedom, which is connected to the motions of the nuclei, from those of the electrons. However, it is important to note that this approximation is not limited to only systems of fixed ions. In fact, the nuclear degree of freedom could be solved once the electronic configuration is known. This approximation was firstly proposed by Born and Oppenheimer. The Born-Oppenheimer Hamiltonian[5] for the electrons can be written as

$$\begin{aligned}
 H_{BO} = & \sum_{i=1}^N \frac{p_i^2}{2m} + \frac{1}{2} \sum_{i,j=1;i \neq j}^N \frac{e^2}{|\vec{r}_i - \vec{r}_j|} \\
 & - \sum_{n=1}^K \sum_{i=1}^N \frac{e^2 Z_n}{|\vec{r}_i - \vec{R}_n|} + \frac{1}{2} \sum_{n,n'=1;n \neq n'}^K \frac{e^2 Z_n Z_{n'}}{|\vec{R}_n - \vec{R}_{n'}|}. \quad (2.2)
 \end{aligned}$$

Never the less, this Hamiltonian is still too complicated to be dealt with. In the next subsection, we introduce a further approximation, known as the one-electron approximation.

2.1.2 One Electron Approximation

The one-electron approximation is based on an assumption that each electron is an independent particle which can be considered separately. Each electron is treated as a particle moving in a mean field potential $U(\vec{r})$. This potential represents the effects of all the other particles in the system. The one-electron equations are of the form

$$\left\{ -\frac{\hbar^2}{2m}\nabla^2 + U_i(\vec{r}) \right\} \psi_i(\vec{r}) = \epsilon_i \psi_i(\vec{r}), \quad (2.3)$$

where $-\hbar^2\nabla^2/2m$ is kinetic energy operator, $\psi_i(\vec{r})$ are the one-electron wave functions and ϵ_i are Lagrange multipliers which arise from the fact that the one-electron wave functions are normalized. Then all $\psi_i(\vec{r})$ can be used as a basis to construct a many-body wave function Ψ . Hartree was two first who consider this approximation.

2.2 Hartree Approximation

This is true only if the electrons are independent particles. We will show that this statement leads to the one-electron approximation. Hartree started that the

N-electrons wave function Ψ is just the product of the one-electron wave functions as

$$\Psi(\vec{r}_1, \vec{r}_2, \dots, \vec{r}_N) = \psi_1(\vec{r}_1)\psi_2(\vec{r}_2)\dots\psi_N(\vec{r}_N), \quad (2.4)$$

where $\psi(\vec{r})$ are obtained from Eq. (2.3). This many-body wave function can be used to find the expectation value of the Hamiltonian as

$$\begin{aligned} \langle \Psi | H | \Psi \rangle &= \sum_{i=1}^N \int d\vec{r} \psi_i^*(\vec{r}) \left(-\frac{\hbar^2}{2m} \nabla^2 + U_i(\vec{r}) \right) \psi_i(\vec{r}) \\ &\quad + \frac{1}{2} \sum_{i=1}^N \sum_{j \neq i}^N \int \frac{e^2}{|\vec{r}_1 - \vec{r}_2|} |\psi_i(\vec{r}_1)|^2 |\psi_j(\vec{r}_2)|^2 d\vec{r}_1 d\vec{r}_2. \end{aligned} \quad (2.5)$$

We introduce a Lagrange multiplier ϵ_i because the one-electron wave functions must be normalized. Then we minimize the above equation with respect to the N-electron wave function, i.e.

$$\frac{\delta}{\delta \Psi} \left\{ \langle \Psi | \hat{H} | \Psi \rangle + \sum_j \epsilon_j \int d\vec{r}_1 |\psi_j(\vec{r}_1)|^2 \right\} = 0. \quad (2.6)$$

This leads to a set of one-electron equations which are known as the Hartree equations

$$\left\{ -\frac{\hbar^2}{2m} \nabla^2 + U_i(\vec{r}) \right\} \psi_i(\vec{r}) = \epsilon_i \psi_i(\vec{r}), \quad (2.7)$$

It can be easily shown that in the Hartree approximation,

$$U_i(\vec{r}) = - \sum_n \frac{e^2 Z_n}{|\vec{r} - \vec{R}_n|} + \sum_{j \neq i} \int d\vec{r}_1 |\psi_j(\vec{r}_1)|^2 \frac{e^2}{|\vec{r} - \vec{r}_1|}. \quad (2.8)$$

The first term is the contribution from the nuclei potentials. The second term is the contribution from the electron potentials which are approximated by the electrostatic interaction among all other electrons and can be written in terms of the electron density $\rho(\vec{r})$. The electron density is constructed from the single electron eigenstates:

$$\rho(\vec{r}) = \sum_{j=1}^N |\psi_j(\vec{r})|^2, \quad (2.9)$$

where the summation over j thus includes all occupied states. Note that, $\psi_j(\vec{r})$ can be solved only when $U_j(\vec{r})$ are known and in return $U_j(\vec{r})$ also depend on all $\psi_j(\vec{r})$. Thus the solution must be solved self-consistently.

2.3 Hartree-Fock Approximation

In Hartree approximation, the effects of particle spin statistics are not included. The way to account for the spin statistics was introduced by Fock.

When we consider a many-electron problem, we must keep in mind that electrons are identical particles and have antisymmetric wave functions. When any two arguments are swapped, the wave function changes sign, for example

$$\Psi(X_1, X_2, \dots, X_i, \dots, X_j, \dots, X_N) = -\Psi(X_1, X_2, \dots, X_j, \dots, X_i, \dots, X_N), \quad (2.10)$$

where X_i contain r representing the electron coordinates and s representing the electron-spin projections. This follows from Pauli exclusion principle which is stated that, no two electrons can have the same set of quantum numbers. It

implies that electrons, which have the same spin, cannot occupy the same state. The probability density for finding particles with specific values of X_1, \dots, X_N is given by

$$\rho(X_1, X_2, \dots, X_N) = |\psi_1(X_1)|^2 |\psi_2(X_2)|^2 \dots |\psi_N(X_N)|^2, \quad (2.11)$$

which is just the product of the one-electron probability densities. This probability distribution is uncorrelated. By taking Pauli principle into account, the wave function can be written in form of Slater determinant, as

$$\Psi_{AS}(X_1, X_2, \dots, X_N) = \frac{1}{\sqrt{N!}} \begin{bmatrix} \psi_1(X_1) & \psi_2(X_1) & \cdots & \psi_N(X_1) \\ \psi_1(X_2) & \psi_2(X_2) & \cdots & \psi_N(X_2) \\ \vdots & \vdots & \ddots & \vdots \\ \psi_1(X_N) & \psi_2(X_N) & \cdots & \psi_N(X_N) \end{bmatrix}. \quad (2.12)$$

We will calculate total energy using this wave function and Hamiltonian. This wave function is also used for finding the expectation value of the Hamiltonian as

$$\begin{aligned} \langle \Psi | \hat{H} | \Psi \rangle &= \sum_i \int d\vec{r} \psi_i^*(\vec{r}) \left(-\frac{\hbar^2}{2m} \nabla^2 + U_i(\vec{r}) \right) \psi_i(\vec{r}) \\ &+ \frac{1}{2} \sum_i \sum_j \int d\vec{r}_1 d\vec{r}_2 \frac{e^2}{|\vec{r}_1 - \vec{r}_2|} |\psi_i(\vec{r}_1)|^2 |\psi_j(\vec{r}_2)|^2 \\ &- \frac{1}{2} \sum_i \sum_{j(\text{like-spin})} \int \int d\vec{r}_1 d\vec{r}_2 \frac{e^2}{|\vec{r}_1 - \vec{r}_2|} \\ &\cdot [\psi_i^*(\vec{r}_1) \psi_j^*(\vec{r}_2) \psi_i(\vec{r}_2) \psi_j(\vec{r}_1)]. \end{aligned} \quad (2.13)$$

The results of minimizing the expectation value of \hat{H} with respect to the one-electron wavefunctions are the Hartree-Fock equations.

$$\begin{aligned}
\epsilon_i \psi_i(\vec{r}) &= \left(-\frac{\hbar^2}{2m} \nabla^2 + U_i(\vec{r}) \right) \psi_i(\vec{r}) \\
&+ \sum_j \int \frac{e^2}{|\vec{r} - \vec{r}_1|} |\psi_j(\vec{r}_1)|^2 \psi_i(\vec{r}) d\vec{r}_1 \\
&- \sum_{j(\text{like-spin})} \int \frac{e^2}{|\vec{r} - \vec{r}_1|} \psi_j^*(\vec{r}_1) \psi_i(\vec{r}_1) \psi_j(\vec{r}) d\vec{r}_1. \quad (2.14)
\end{aligned}$$

The first two terms is kinetic energy and the effective potential. The second term is the Hartree potential and the third term is the exchange term. The effects of the exchange term are that the electrons of like spins tend to avoid each other. As a result, an electron has a “hole” associated with it. This hole is known as the exchange hole. It is a small volume around the electron which other like spin electrons try to avoid. The charge, which fills in the exchange hole, is positive and equivalent to the absence of one-electron.

2.4 Density Functional Approximation

A weakness of the Hartree-Fock equations is that they depends on the occupied electron orbitals. Thus it is difficult to apply for an extended system. A better way to solve this problem is called the density functional approximation introduced by Hohenberg, Kohn and Sham. In the density functional approximation, Schrödinger equations depend on the electron density rather than on the individual electron orbital. This method can include correlation effects which are completely neglected in the Hartree-Fock approximation.

Kohn and Sham[9] stated, based on the Hohenberg-Kohn theorem, that energy of the system $E(\rho(\vec{r}))$ is a function of the electron density. and can be minimized by varying the density as

$$\frac{\delta}{\delta\rho(\vec{r})} \left\{ E(\rho(\vec{r})) - \epsilon \int \rho(\vec{r}) d\vec{r} \right\} = 0. \quad (2.15)$$

We get

$$\frac{\delta E(\rho(\vec{r}))}{\delta\rho(\vec{r})} = \epsilon,$$

and

$$\int \rho(\vec{r}) d\vec{r} = N.$$

The variation principle for interacting electrons takes the form:

$$\begin{aligned} E(\rho(\vec{r})) &= T_s(\rho(\vec{r})) + \frac{1}{2} \int \int \frac{\rho(\vec{r})\rho(\vec{r}_1)}{|\vec{r} - \vec{r}_1|} d\vec{r}d\vec{r}_1 \\ &+ E_{xc}(\rho(\vec{r})) + \int \rho(\vec{r}) V_{xc} d\vec{r}, \end{aligned} \quad (2.16)$$

where $T_s(\rho(\vec{r}))$ is the kinetic energy of non interacting electron gas with density $\rho(\vec{r})$. It is written in the form

$$T_s(\rho(\vec{r})) = -\frac{\hbar^2}{2m} \sum_i \int \psi_i^*(\vec{r}) \nabla^2 \psi_i(\vec{r}) d\vec{r}. \quad (2.17)$$

E_{xc} is the exchange-correlation energy and is V_{xc} the exchange-correlation potential. The second, third and fourth terms of Eq. (2.16) are the Hartree energy, exchange-correlation energy and external energy respectively. The corresponding

Euler-Lagrange equation for a given total number of electrons have the form

$$\frac{\delta T_s(\rho(\vec{r}))}{\delta \rho(\vec{r})} + V_{eff}(\vec{r}) = \epsilon, \quad (2.18)$$

where

$$V_{eff}(\vec{r}) = V_{ion}(\vec{r}) + \int \frac{\rho(\vec{r}')}{|\vec{r} - \vec{r}'|} d\vec{r}' + V_{xc}(\vec{r}), \quad (2.19)$$

and

$$V_{xc}(\vec{r}) = \frac{\delta E_{xc}(\rho(\vec{r}))}{\delta \rho(\vec{r})}. \quad (2.20)$$

V_{eff} is the effective potential and V_{ion} is nuclei potential. Eq. (2.18) is the solution of the one-electron equation in an effective external potential $V_{eff}(\vec{r})$.

The minimized density is given by solving the single electron equation, called the Kohn-Sham equation,

$$\left(-\frac{\hbar^2}{2m} \nabla^2 + V_{eff}(\vec{r}) \right) \psi_i(\vec{r}) = \epsilon_i \psi_i(\vec{r}), \quad (2.21)$$

with

$$\rho(\vec{r}) = \sum_i |\psi_i(\vec{r})|^2,$$

and the total energy of the system is

$$E = \sum_i \epsilon_i - \frac{1}{2} \int d\vec{r} d\vec{r}_1 \rho(\vec{r}) \frac{e^2}{|\vec{r} - \vec{r}_1|} \rho(\vec{r}_1) + E_{xc}[\rho(\vec{r})] - \int d\vec{r} V_{xc\rho}[(\vec{r})] \rho(\vec{r}). \quad (2.22)$$

Again $\psi_i(\vec{r})$ can be solved only if we know $V_{eff}(\vec{r})$ and $V_{eff}(\vec{r})$ is a function of $\psi_i(\vec{r})$. Thus these equations must be solved self consistently. This scheme

naturally leads to an iterative procedure. Firstly a starting electronic density is guessed and the refined through the self consistent cycle below.

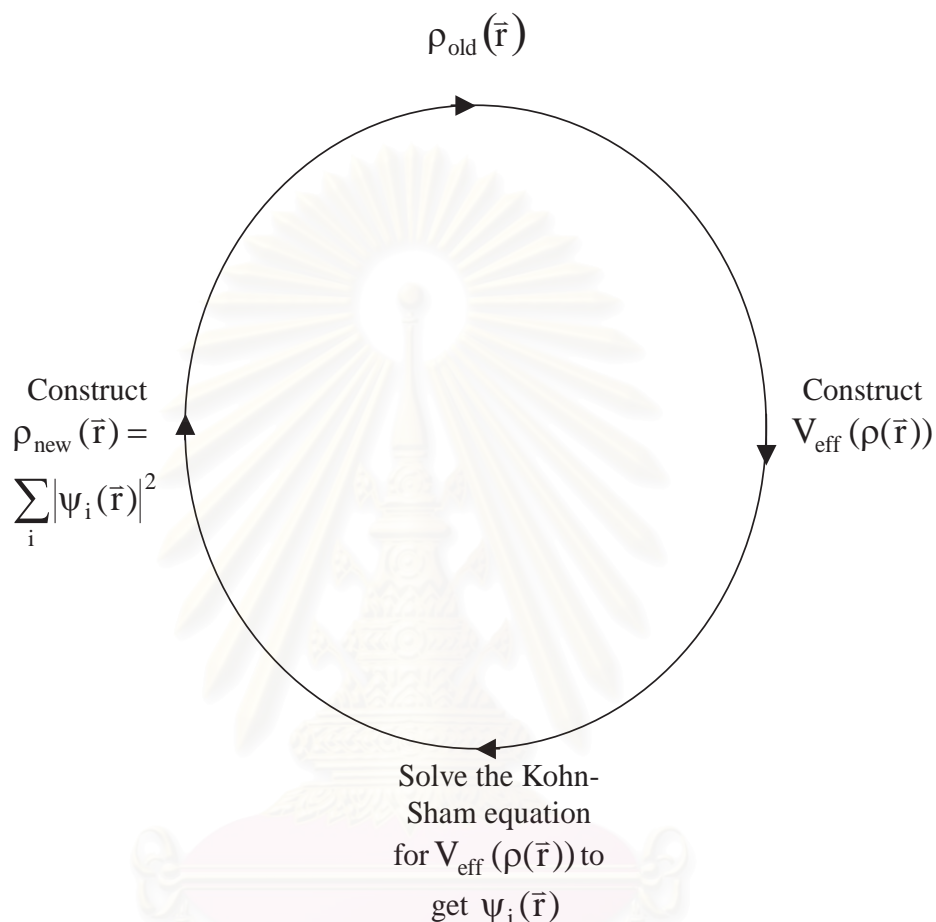


Fig. 2.1 A self-consistent method used in the density functional theory.

2.4.1 Local Density Approximation (LDA)

The difference between the Hartree-Fock approximation and the density functional approximation is that the Hartree-Fock exchange term is replaced by the exchange-correlation energy which is a function of the electron density. For a ho-

homogeneous electron gas, the exchange-correlation potential is a functional derivative of the exchange-correlation energy with respect to the local density. To a good approximation the exchange-correlation potential at position \vec{r} depends only on the electron density at position \vec{r} . This is called local density approximation (LDA)[5]. In a nonhomogeneous system, it depends not only on the density at \vec{r} but also on its variation close to \vec{r} . The explicit local density approximation expression for the exchange-correlation energy is

$$E_{xc}(\rho(\vec{r})) \approx \int \epsilon_{xc}(\rho(\vec{r}))(\rho(\vec{r})) d\vec{r}, \quad (2.23)$$

where $\epsilon_{xc}(\rho(\vec{r}))$ is the exchange-correlation energy per electron of the uniform electron gas of density $\rho(\vec{r})$. The exchange energy per electron can be written in the form of

$$\epsilon_{ex}(\rho(\vec{r})) = -\frac{3e^2}{4} \left(\frac{3}{\pi}\right)^{\frac{1}{3}} (\rho(\vec{r}))^{\frac{1}{3}}, \quad (2.24)$$

and the local density exchange potential is given by

$$V_{ex}(\rho(\vec{r})) = -2e^2 \left(\frac{3}{\pi}\right)^{\frac{1}{3}} (\rho(\vec{r}))^{\frac{1}{3}}. \quad (2.25)$$

The local density approximation is remarkably accurate but often fails when the electrons are strongly correlated, such as a system containing d and f electron orbitals.

Chapter 3

The Wigner-Seitz Method

3.1 Introduction

The purpose of this chapter is to present a simple calculation of the ground state energy of solid metallic hydrogen using the Hartree-Fock approximation. The wave functions of electrons in the hydrogen metal can be determined by the Wigner-Seitz method, some times called the Cellular method, which was first proposed by Wigner and Seitz. The Wigner-Seitz method[4], reduces a many-electron problem into one-electron problems and gives the dispersion of the energy band near $k = 0$. The interactions between a given proton and an electron are modelled by a Coulomb potential, a uniform screened Coulomb potential and a Thomas-Fermi screened potential. The correlation effect is included by using the most acceptable correlation potential[6].

3.2 The Cellular Method

In general a metal is composed of N ion cores and N electrons moving around these ion cores. Ideally, a solid has a periodic symmetry in the bulk. This fact can be exploited to reduce the size of the problem by using Bloch's theorem[10]. Bloch's theorem enables us to replace the problem of solving the Schrödinger equation for an infinite periodic solid by a problem of solving the Schrödinger equation in a unit cell with different Bloch boundary conditions. In order to obtain the simplest boundary conditions, we choose the unit cell to be a polyhedron with greatest possible symmetry about an atomic position. Some examples are shown in Fig. 3.1.

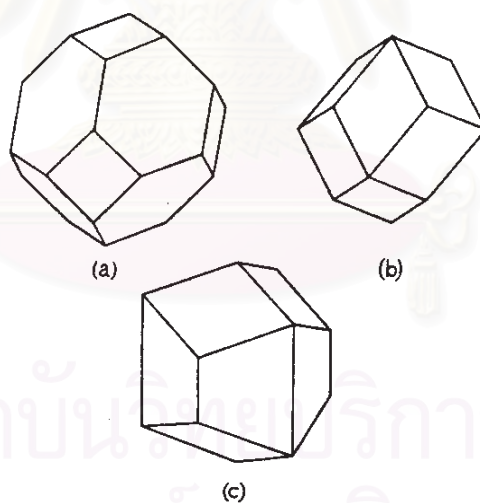


Fig. 3.1 Atomic polyhedra for (a) the body-centered cubic lattice, (b) the face-centered cubic lattice, (c) the hexagonal close-packed lattice.

Thus the whole metal can be divided into N atomic cells with an equal volume. For simplicity, a volume of an atomic cell V is replaced by a sphere of radius r_s where $\frac{4}{3}\pi r_s^3 = V$. This sphere is called Wigner-Seitz's sphere. The key physics of this method is that even though electrons are nearly free to move but on the average, one Wigner-Seitz's sphere contains only one electron. In fact there can be only two electrons with opposite spins in each orbital states $\psi_k(\vec{r})$. The resulting Hartree-Fock like approximation for the ground state energy is just

$$\begin{aligned}
NE_0 = & 2 \sum_k \int \psi_k^*(\vec{r}) \left[-\frac{\hbar^2}{2m} \nabla^2 + \sum_a^N U_a(\vec{r}) \right] \psi_k(\vec{r}) d\vec{r} \\
& + 2 \sum_k \sum_{k'} \int \int \frac{e^2}{|\vec{r}_1 - \vec{r}_2|} |\psi_k(\vec{r}_1)|^2 |\psi_{k'}(\vec{r}_2)|^2 d\vec{r}_1 d\vec{r}_2 \\
& - \sum_k \sum_{k'} \int \int \frac{e^2}{|\vec{r}_1 - \vec{r}_2|} \psi_k^*(\vec{r}_1) \psi_{k'}^*(\vec{r}_2) \psi_k(\vec{r}_2) \psi_{k'}(\vec{r}_1) d\vec{r}_1 d\vec{r}_2 \\
& + \frac{1}{2} \sum_a^N \sum_{b \neq a}^N \frac{e^2}{|\vec{R}_a - \vec{R}_b|}, \tag{3.1}
\end{aligned}$$

where $U_a(r)$ is potential between an electron and its ion core within cell a and $U_a(r) = 0$ outside the cell, E^0 is the average energy per electron and the last term is the interaction energy between a proton at position R_a in Wigner-Seitz cell a and a proton at position R_b in Wigner-Seitz cell b . The wave functions $\psi_k(\vec{r})$ are eigenfunctions of the Schrödinger equation

$$\left[-\frac{\hbar^2}{2m} \nabla^2 + U(\vec{r}) \right] \psi_k(\vec{r}) = \epsilon(k) \psi_k(\vec{r}), \tag{3.2}$$

where the potential function $U(\vec{r})$ between electrons and their corresponding ion cores in Eq.(3.1) can be written as

$$U(\vec{r}) = \sum_{a=1}^N U_a(\vec{r}).$$

$U_a(\vec{r})$ are assumed spherically symmetric. This is called spherical cell approximation. Explicit potentials will be discussed in next section. By replacing Eq.(3.2) in Eq.(3.1), each integral over the volume in the first and the second terms in Eq.(3.1) may be separated into a sum over lattice sites plus an integral over the corresponding Wigner-Seitz cells. The problem is reduced from N electron problem to N one-electron problems which are much easier to be solved. In spherical cell approximation, all cross terms in the integral of the first and the second term, in Eq.(3.1), conspire to exactly cancel with the proton-proton energy. Throughout this work, the ground state energy E^0 is expressed in atomic unit. In this unit an energy is expressed in rydberg($1Ry = me^4/2\hbar$) and length in Bohr unit($1a_0 = \hbar^2/me^2$). Consequently, we let $me^4/2\hbar = 1$, $\hbar^2/me^2 = 1$, $\hbar^2/2m = 1$ and $e^2 = 2$.

$$NE^0 = 2 \sum_k \epsilon(k) + 2 \sum_k \sum_{k'} \int_a \int_a \frac{2}{|\vec{r}_1 - \vec{r}_2|} |\psi_k(\vec{r}_1)|^2 |\psi_{k'}(\vec{r}_2)|^2 d\vec{r}_1 d\vec{r}_2 - \sum_k \sum_{k'} \int \int \frac{2}{|\vec{r}_1 - \vec{r}_2|} \psi_k^*(\vec{r}_1) \psi_{k'}^*(\vec{r}_2) \psi_k(\vec{r}_2) \psi_{k'}(\vec{r}_1) d\vec{r}_1 d\vec{r}_2 \quad (3.3)$$

This final expression is called the Wigner-Seitz approximation. The wave functions and the energy, which is a function of k , can be determined. The exact

wave functions are complicated because they are expressed by some functions of complex number and their true symmetry is not known. However, one hydrogen atom has only one electron, when it forms a metal, the conduction band is only half-band filled. Thus the expansion of the wave function near the bottom of the band can be expressed as[11]

$$\psi_k(r) = e^{i\vec{k}\cdot\vec{r}} \{u_0(r) + u_1(r)k + u_2(r)k^2 + \dots\}. \quad (3.4)$$

In addition, the energy band dispersion $\epsilon(k)$, which is the most important relation because it leads to the ground state energy, is

$$\epsilon(k) = E_0 + E_2k^2 + E_4k^4 + \dots \quad (3.5)$$

Due to the periodic nature of metals, the wave functions must satisfy Bloch conditions and the metallic condition, i.e. the electrons are not truly localized in Wigner-Seitz spheres but rather wandering around, and hence $(d\psi/dr)_{r_s} = 0$. This principle is also applied for the metallic hydrogen.

We can separate the Schrödinger equation,

$$(-\nabla^2 + U(r)) \psi_k(r) = \epsilon(k) \psi_k(r), \quad (3.6)$$

into a set of equations by substituting the expansion of the wave functions and the energy dispersion as follows,

$$(-\nabla^2 + U - E_0) u_0 = 0,$$

$$\begin{aligned}
(-\nabla^2 + U - E_0) u_1 &= 2i \frac{\partial u_0}{\partial z}, \\
(-\nabla^2 + U - E_0) u_2 &= 2i \frac{\partial u_1}{\partial z} + (E_2 - 1) u_0, \\
(-\nabla^2 + U - E_0) u_{2n} &= 2i \left(\frac{\partial u_{2n-1}}{\partial z} \right) + (E_2 - 1) u_{2n-2} + \dots + E_{2n} u_0, \\
(-\nabla^2 + U - E_0) u_{2n+1} &= 2i \left(\frac{\partial u_{2n}}{\partial z} \right) + (E_2 - 1) u_{2n-1} + \dots + E_{2n} u_1.
\end{aligned} \tag{3.7}$$

Bardeen[12] and Silverman[13] showed that the first few terms and E_0, E_2 and E_4 were given by solving the boundary condition, $(\partial (s_part_of_u_{2n}) / \partial r)_{r=r_s} = 0$. As a result, we get

$$E_2 = \gamma \left(\frac{r}{f_1} \frac{\partial f_1}{\partial r} \right)_{r_s}, \tag{3.8}$$

$$E_4 = \frac{2}{5} r_s^2 E_2 - \frac{4 r_s^2 E_2^2 E_0}{15 \gamma} \left(\frac{r}{f_2} \frac{\partial f_2}{\partial r} \right)_{r_s}^{-1} + \frac{\gamma E_2}{u_0(r_s)} \left(\frac{\partial^2 f_1}{\partial r \partial E} \right)_{r_s, E_0}, \tag{3.9}$$

where $\gamma = \frac{4}{3} \pi r_s^3 u_0^2(r_s)$ and

$$\left(-\frac{1}{r^2} \frac{d}{dr} r^2 \frac{d}{dr} + U(r) - E_0 \right) u_0 = 0, \tag{3.10}$$

and f_l satisfies the following equation

$$\left(-\frac{1}{r^2} \frac{d}{dr} r^2 \frac{d}{dr} + U(r) + \frac{l(l+1)}{r^2} - E_0 \right) f_l = 0, \tag{3.11}$$

where index $l = 0, 1, 2, 3, \dots$. In the usual atomic physics, l is called the quantum number of the orbital angular momentum and f_l is the radial part of the corresponding wave function. However, the physical interpretation of f_l in above equation is quite different. It just a dummy function related to u_l in Eq.(3.4).

$\psi(r)$ must also satisfy $(\partial\psi/\partial r)_{r_s} = 0$. the complete relation between f_1 and u_0 is $f_1(r_s) = r_s u_0(r_s)$ [13]. The first term in Eq.(3.3) may be evaluated by replacing the sum by an integral over the Fermi sphere. For the final result, we get

$$\frac{2}{N} \sum_k \epsilon(k) \approx E_0 + E_2 \frac{2.21}{r_s^2} + E_4 \frac{5.81}{r_s^4}, \quad (3.12)$$

In next section, we will specify some potentials for the metallic hydrogen. Once, an explicit potential function $U(r)$ is applied, the function u_0, f_1 and f_2 can be evaluated. The ground state energy in Eq.(3.3) can also be calculated. In previous work, Styer and Ashcroft[7] have evaluated u_0 and f_1 , and used Eq.(3.3) to calculate the ground state energy of metallic hydrogen. The exact calculation is far more complicated so they preformed some sensible estimation to all terms in Eq.(3.3). Nevertheless, they evaluated the first term in Eq.(3.3) by expanding $\epsilon(k)$ up to k^2 only. In this work, we shall evaluate f_2 and perform a more accurate calculation by adding a correction term of order k^4 to $\epsilon(k)$.

3.3 Model Potentials

3.3.1 Coulomb Potential

In this section, we assume that the interaction between the electron and its positive core is purely coulomb, *i.e.* $U(r) = -2/r$. This means that the nuclei interact with all other nuclei in the metal because this potential is long range.

According to our calculation, we find that[7]

$$u_0(r) = C e^{-\sqrt{\epsilon_b} r} \left\{ {}_1F_1 \left(1 - \frac{1}{\sqrt{\epsilon_b}}; 2; 2\sqrt{\epsilon_b} r \right) \right\}, \quad (3.13)$$

$$f_1(r) = A r e^{-\sqrt{\epsilon_b} r} \left\{ {}_1F_1 \left(2 - \frac{1}{\sqrt{\epsilon_b}}; 4; 2\sqrt{\epsilon_b} r \right) \right\}, \quad (3.14)$$

$$f_2(r) = A_1 r^2 e^{-\sqrt{\epsilon_b} r} \left\{ {}_1F_1 \left(3 - \frac{1}{\sqrt{\epsilon_b}}; 6; 2\sqrt{\epsilon_b} r \right) \right\}, \quad (3.15)$$

where $\epsilon_b = -E_0$ and ${}_1F_1$ is the confluent hypergeometric function or Kummer function[14] which is written in form

$${}_1F_1(a, b, r) = 1 + \frac{a}{b} r + \frac{a(a+1)}{2!b(b+1)} r^2 + \frac{a(a+1)(a+2)}{3!b(b+1)(b+2)} r^3 + \dots$$

A, A_1 are an arbitrary constant which is cancelled in Eq.(3.8) and (3.9) and C is normalized constant.

3.3.2 Screening Effects

As electrons move nearly freely in metals, the screening effects are extremely efficient. In order to study the metallic hydrogen, we must consider the screening effects as well. Thus, our calculations are more realistic if we replace Coulomb potential by a screened potential. Our Hamiltonian is modified and the Hartree-Fock like energy must include a negative term,

$$-2 \sum_k \int_a |\psi_k(\vec{r})|^2 U_s(\vec{r}) d\vec{r}.$$

where $U_s(\vec{r})$ is screened potential and is assumed spherically symmetric.

For the uniform screening, which is the potential of a negative unit charge uniformly distributed throughout the Wigner-Seitz sphere, the potential is

$$U(r) = -\frac{2}{r} + U_s(r) = -\frac{2}{r} + \frac{(3r_s^2 - r^2)}{r_s^3}. \quad (3.16)$$

The uniform screened potential is short range. The potential vanishes at the cell boundary. This means that the nuclei do not feel the presence of the others. By inserting this potential in Eq. (3.10) and solving by using the Frobenius method¹, we find that[7]

$$u_0(r) = \frac{C}{r} \sum_{i=1}^{\infty} b_i r^i, \quad (3.17)$$

where C is the normalized constant,

$$b_0 = 0, b_1 = 1, b_2 = -1, b_3 = \frac{1}{6} (2 - E_0 + 3/r_s),$$

and

$$b_i = \frac{1}{(i-1)} \left(2b_{i-1} + \left(E_0 - \frac{3}{r_s} \right) b_{i-2} + \frac{b_{i-4}}{r_s^3} \right), i \geq 4.$$

The solutions f_1, f_2 of Eq.(3.11) are also solved. We get

$$f_1 = \frac{A}{r} \sum_{i=1}^{\infty} b_i r^i, \quad (3.18)$$

where

$$b_0 = 0, b_1 = 0, b_2 = 1, b_3 = -\frac{1}{2},$$

¹A solution of a differential equation $y(x)$ is expanded in a Taylor's series about regular singular point x_0 , $y(x) = \sum_{n=0}^{\infty} a_n (x - x_0)^{m+n}$. Then, the coefficient of the polynomial a_n are determined.

and

$$b_i = \frac{1}{i(i-1)-2} \left(2b_{i-1} + \left(E_0 - \frac{3}{r_s} \right) b_{i-2} + \frac{b_{i-4}}{r_s^3} \right), i \geq 4.$$

and

$$f_2 = \frac{A_1}{r} \sum_{i=1}^{\infty} b_i r^i, \quad (3.19)$$

where

$$b_0 = 0, b_1 = 0, b_2 = 0, b_3 = 1,$$

and

$$b_i = \frac{1}{i(i-1)-6} \left(2b_{i-1} + \left(E_0 - \frac{3}{r_s} \right) b_{i-2} + \frac{b_{i-4}}{r_s^3} \right), i \geq 4.$$

For Thomas-Fermi screening, the potential is

$$U(r) = -\frac{2}{r} + U_s(r) = -\frac{2}{r} + \frac{2}{r} (1 - e^{-k_{TF}r}), \quad (3.20)$$

where $k_{TF} = \left(\sqrt[3]{12/\pi} \right) / \sqrt{r_s}$. Thomas-Fermi screened potential has an intermediate range. The potential extends over a couple of neighboring cells. By inserting Eq. (3.20) into Eq. (3.10) and using the Frobenius method, the solution of u_0 is[7]

$$u_0 = \frac{C_1}{r} \sum_{i=1}^{\infty} b_i r^i \quad (3.21)$$

where

$$b_0 = 0, b_1 = 1,$$

and

$$b_i = \frac{1}{i(i-1)} \left(2 \sum_{m=1}^{i-1} \frac{-k_{TF}^{i-m-1}}{(i-m-1)} b_m + E_0 b_{i-2} \right), i \geq 2.$$

The solutions of f_1, f_2 are

$$f_1 = \frac{A_2}{r} \sum_{i=1}^{\infty} b_i r^i \quad (3.22)$$

where

$$b_0 = 0, b_1 = 1,$$

and

$$b_i = \frac{1}{i(i-1)-2} \left(2 \sum_{m=1}^{i-1} \frac{-k_{TF}^{i-m-1}}{(i-m-1)} b_m + E_0 b_{i-2} \right), i \geq 2,$$

$$f_2 = \frac{A_3}{r} \sum_{i=1}^{\infty} b_i r^i \quad (3.23)$$

where

$$b_0 = 0, b_1 = 0, b_2 = 1,$$

and

$$b_i = \frac{1}{i(i-1)-6} \left(2 \sum_{m=1}^{i-1} \frac{-k_{TF}^{i-m-1}}{(i-m-1)} b_m + E_0 b_{i-2} \right), i \geq 3.$$

Again, A, A_1, A_2 and A_3 in Eq. (3.18), (3.19), (3.22) and (3.23) are an arbitrary constant which is cancelled in Eq. (3.8) and (3.9) and C and C_1 in Eq.(3.17) and (3.21) are a normalized constant.

By substituting u_0, f_1 and f_2 into Eq. (3.8) and (3.9), we can calculate the energy dispersion $\epsilon(k)$, its average over the conduction band in Eq. (3.12) and the ground state energy in Eq.(3.3).

3.4 Hartree Energy

We have seen that the wave functions of the occupied states are nearly free. Let us therefore use the free electron approximation to evaluate the remaining two terms of Eq. (3.3). Since these terms have opposite signs, it is probable that the errors introduced in this way will partially cancel each other. Now we investigate the second term in Eq. (3.3) which is called Hartree energy. The first term in the sum of Hartree energy for the lower bound is

$$\begin{aligned} H_{00} &= \int_a \int_a \frac{u_0^2(\vec{r}_1) u_0^2(\vec{r}_2)}{|\vec{r}_1 - \vec{r}_2|} d\vec{r}_1 d\vec{r}_2, \\ &= 32\pi^2 \int^{r_s} dr r u_0^2(r) \int^r dr' r'^2 u_0^2(r'), \end{aligned} \quad (3.24)$$

where $u_0(r)$ is obtained from Eq. (3.7). It is the Hartree energy at wave vector $k = 0$. In the free electron approximation, $\rho(r) = \frac{N}{V} = \frac{3}{4\pi r_s^3}$, so the last term in the sum for the upper bound is[7]

$$\begin{aligned} H_{k_F k_F} &= 32\pi^2 \int^{r_s} dr r \int^r dr' r'^2 \left(\frac{3}{4\pi r_s^3} \right)^2, \\ &= \frac{1.2}{r_s} Ry. \end{aligned} \quad (3.25)$$

This is Hartree energy at the Fermi level. The Hartree energy is approximated as the average between the two bounds.

3.5 Exchange Energy

Again, the third term in Eq. (3.3), called the exchange energy, is evaluated by using the wave function of the free electron. The plane wave is substituted in the equation and a summation is replaced by an integral over the Fermi sphere. This gives[15]

$$\begin{aligned}
 \sum_k \epsilon_x(k) &= -\frac{2}{2\pi} \left[2k_F + \frac{k_F^2 - k}{k} \log \left(\frac{k_F + k}{k_F - k} \right) \right] \\
 &= -\frac{V}{\pi 8\pi^3} \int_0^{k_F} \left[2k_F + \frac{k_F^2 - k}{k} \log \left(\frac{k_F + k}{k_F - k} \right) \right] 4\pi k^2 dk \\
 &= -\frac{V}{2\pi^3} \int_0^{k_F} \left[2k_F k^2 + k (k_F^2 - k^2) \log \left(\frac{k_F + k}{k_F - k} \right) \right] dk \\
 &= -\frac{0.916N}{r_s} Ry. \tag{3.26}
 \end{aligned}$$

where N is a number of the electron.

3.6 Correlation Energy

To further improve the accuracy of the ground state energy, an accurate correlation energy ϵ_c is added to Eq. (3.3). The explicit expression for the correlation energy per electron is[6],[16]

$$\begin{aligned}
 \epsilon_c(r_s) &= A \left\{ \ln \left(\frac{x^2}{X(x)} \right) + \frac{2b}{Q} \arctan \left(\frac{Q}{2x+b} \right) - \right. \\
 &\quad \left. \frac{bx_0}{X(x_0)} \left[\ln \left(\frac{(x-x_0)^2}{X(x)} \right) + \frac{2(b+2x_0)}{Q} \arctan \left(\frac{Q}{2x+b} \right) \right] \right\} \tag{3.27}
 \end{aligned}$$

where $x = \sqrt{r_s}$, $X(x) = x^2 + bx + c$, $Q = \sqrt{4c - b^2}$, $A = 0.0621814$, $x_0 = -0.10498$, $b = 3.72744$ and $c = 12.9352$. This correlation energy was proposed by Ceperley and Alder[6] and revived by Vosko, Wilk and Nusair and accepted as the most accurate correlation energy available.

Finally, the addition term in the screened potential case is approximated in the same manner as the Hartree energy, i.e. by averaging between the lower bound, (H_0), and upper bound, (H_{k_F}). The lower bound is

$$H_0 = -4\pi \int^{r_s} dr u_0^2(r) U_s(r). \quad (3.28)$$

The upper bound for uniform screening is

$$H_{k_F} = -\frac{3}{r_s} \int^{r_s} dr r^2 U_s(r) = -\frac{12}{5r_s}, \quad (3.29)$$

and for the Thomas-Fermi screening, the upper bound is[7]

$$H_{k_F} = -\frac{3}{r_s} \int^{r_s} dr r^2 U_s(r) = -\frac{6}{3} \left[\frac{r_s^2}{2} - \frac{1}{k_{TF}} + e^{-k_{TF} r_s} \left(\frac{r_s}{k_{TF}} + \frac{1}{k_{TF}^2} \right) \right]. \quad (3.30)$$

The total ground state energy per electron is evaluated by replacing the sum by an integral over the Fermi sphere. Finally, in Wigner-Seitz approximation, the total ground state energy is expressed as

$$\begin{aligned} E^0(r_s) = & E_0 + E_2 \frac{2.21}{r_s^2} + E_4 \frac{5.81}{r_s^4} + \frac{1}{2} (H_{00} + H_{k_F k_F}) \\ & + \frac{1}{2} (H_0 + H_{k_F}) - \frac{0.916}{r_s} + \epsilon_c(r_s). \end{aligned} \quad (3.31)$$

However, a fundamental weakness of this approach is that the higher order terms in k and the direction dependence of the wave function are discarded. The directional dependency can be neglected if the lattice has high symmetry such as body-centered cubic. In the next chapter, we will introduce a more complicated and more accurate method for calculating the total ground state energy where the effects of lattice structures are fully included.



สถาบันวิทยบริการ
จุฬาลงกรณ์มหาวิทยาลัย

Chapter 4

The Full Potential Linearized Augmented Plane Wave

4.1 Introduction

A fundamental weakness of Wigner-Seitz method is that the higher order terms in k and the direction dependence of the wave function are discarded and the atomic polyhedral cell is replaced by a sphere of radius r_s . The total ground state energy depends on the density of the metal but not on the information of the lattice structure. In addition, the Hartree-Fock approximation completely neglects correlation effects and the assumption in the part of Hartree and exchange energies is that wave function of system is of nearly free electrons. To improve our work in chapter 3, in this chapter an alternative method, which can calculate the ground state energy, the energy band, the density of states and other properties of metals under various lattice structures is discussed. This method is called the full potential linearized augmented plane wave method (FP-LAPW), which is the

most accurate methods available for performing electronic structure calculations for crystals. It is based on the density functional theory. For the treatment of the exchange and correlation, we use the local density approximation. Normally, many-electron problems in metals can be simplified by solving self consistently a one-electron problem, known as Kohn-Sham equation. The Kohn-Sham equation is solved by using the variational method. In this method, stationary states of the wave function are found within a subspace of Hilbert space[17] that is spanned by a set of basis vectors

$$|\psi\rangle = \sum_p C_p |\chi_p\rangle, \quad (4.1)$$

where χ_p is a set of basis vectors and C_p is coefficient which is the projection of ψ onto the basis vector χ_p . The energy functional is given by

$$E = \frac{\sum_{p,q=1}^N C_p^* C_p H_{pq}}{\sum_{p,q=1}^N C_p^* C_p O_{pq}}, \quad (4.2)$$

with Hamiltonian matrix defined by

$$H_{pq} = \langle \chi_p | H | \chi_q \rangle, \quad (4.3)$$

and the overlap matrix,

$$O_{pq} = \langle \chi_p | \chi_q \rangle. \quad (4.4)$$

4.2 The Augmented Plane Wave(APW)

There are two things to strive for when we choose a basis set. First of all the basis functions should be as mathematically simple as possible, in order to simplify the setup of the matrix elements. The other important feature is that the basis functions are well suited to describe the system of interest. This will minimize the size of basis set and hence the computation effort. The augmented plane wave (APW)[18-19] was originated in 1937 by J.C. Slater. The APW is based on the muffin tin approximation to the actual crystal potential. Firstly, we construct a sphere centered at each atomic site. Inside the sphere, there is a potential which is spherically symmetric and labelled by I . Outside the sphere the potential is taken to be a constant, usually zero, labelled by II . In this work, the radius of the muffin tin sphere is chosen to be one-half the nearest neighbor distance.

สถาบันวิทยบริการ
จุฬาลงกรณ์มหาวิทยาลัย

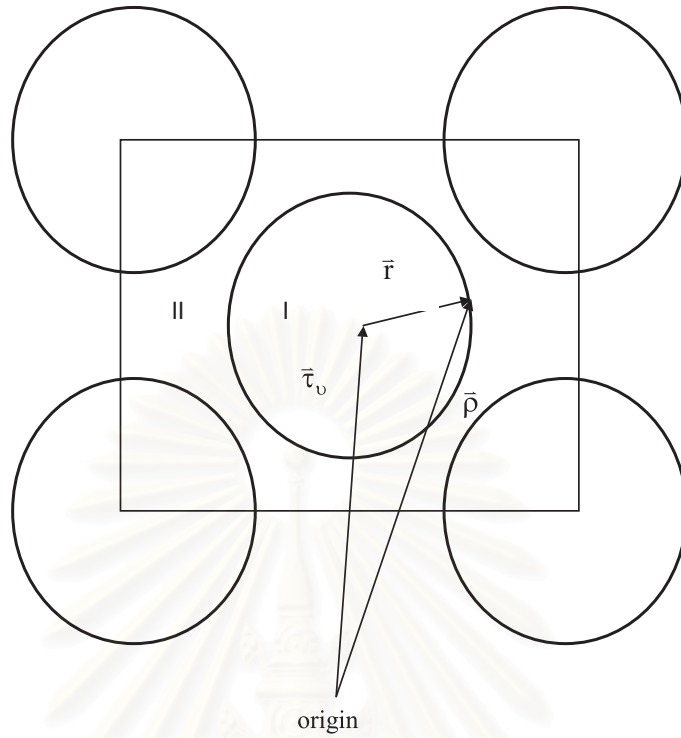


Fig. 4.1 The muffin tin potential approximation used in the augmented plane waves. $\vec{\tau}_v$ is a position of each atom, \vec{r} is a local coordinate in the sphere, centered at the atom position, and $\vec{\rho}$ is a position vector which relative to origin and can be expressed as $\vec{\rho} = \vec{\tau}_v + \vec{r}$.

The two types of different regions have different basis sets. Inside the non-overlapping atomic sphere v of radius R_v there is a basis χ_k^I in the form of linear combination of radial functions and spherical harmonics.

$$\chi_k^I(r, E) = \sum_{l=0}^{\infty} \sum_{m=-l}^l A_{lm}(k) u_l(r, E) Y_m^l(\hat{r}), \quad (4.5)$$

where A_{lm} is a coefficient, $Y_m^l(\hat{r})$ is spherical harmonic and the functions $u_l(r, E)$ are solutions of the radial Schrodinger equation with energy E ,

$$-\frac{1}{r^2} \frac{d}{dr} \left(r^2 \frac{du_l(r, E)}{dr} \right) + \left[\frac{l(l+1)}{r^2} + U_v(r) \right] u_l(r, E) = E u_l(r, E). \quad (4.6)$$

It is regular at the origin and can be solved with high accuracy. $U_v(r)$ is a spherically symmetric potential. In the region outside the sphere or the interstitial region a plane wave expansion is used, i.e.

$$\chi_k^{II} = \frac{1}{\sqrt{V}} e^{i\vec{k} \cdot \vec{\rho}} = \frac{1}{\sqrt{V}} e^{i\vec{k} \cdot \vec{\tau}_v} e^{i\vec{k} \cdot \vec{r}}, \quad (4.7)$$

where $\vec{k}_n = \vec{k} + \vec{K}_n$, \vec{K}_n are the reciprocal lattice vectors, \vec{k} is the wave vector inside the first Brillouin zone, V is the volume of unit cell and vector \vec{r} , $\vec{\rho}$, $\vec{\tau}_v$ are showed in the Fig.4.1. Each plane wave is augmented by an atomic-like function in every atomic sphere. The coefficients $A_{lm}(k)$ is determined by boundary conditions stated that the wave functions in both regions are matched at the muffin tin radius. However, the slope of the wave functions at muffin tin radius does not necessarily continuous. The plane wave can be expanded in spherical harmonics as,

$$\frac{1}{\sqrt{V}} e^{i\vec{k} \cdot \vec{\rho}} = \frac{4\pi}{\sqrt{V}} e^{i\vec{k} \cdot \vec{\tau}_v} \sum_{l=0}^{\infty} \sum_{m=-l}^l i^l j_l(kr) Y_m^{l*}(\hat{k}) Y_m^l(\hat{r}), \quad (4.8)$$

where $i = \sqrt{-1}$, $j_l(x)$ is a spherical Bessel function of order l . Otherwise, the unit vector \hat{k} and \hat{r} are the angular of vectors \vec{k} and \vec{r} respectively. From the

boundary conditions, the coefficients are

$$A_{lm} = \frac{4\pi}{\sqrt{V}} e^{i\vec{k}\cdot\vec{\tau}_v} i^l Y_m^{l*}(\hat{k}) \frac{j_l(kR_v)}{u_l(R_v)}, \quad (4.9)$$

where R_v the radius of the muffin tin sphere.

In summary the APW function for the state, which is specified by the wave vector \vec{k} , has the following form,

$$\chi^{APW}(\vec{k}, \vec{r}) = \frac{1}{\sqrt{V}} e^{i\vec{k}\cdot\vec{r}}; r \in II \quad (4.10)$$

$$= \frac{4\pi}{\sqrt{V}} e^{i\vec{k}\cdot\vec{\tau}_v} \sum_{lm} i^l j_l(kR_v) Y_m^{l*}(\hat{k}) Y_m^l(\hat{r}) \frac{u_l(r)}{u_l(R_v)}; r \in I \quad (4.11)$$

where l values have a cut off at finite value. The wave functions can be expanded in terms of APW basis set as,

$$\psi_n(k, r) = \sum_p C_p^n \chi_p^{APW}, \quad (4.12)$$

where C_p^n is coefficient which is the projection of $\psi_n(k, r)$ onto the basis vector χ_p^{APW} . The C_p summation is over the reciprocal lattice vectors \vec{K}_p which have norm smaller than some cut off. The variational method is applied on the wave functions which are expanded by using the APW basis set for minimizing the energy with respect to each coefficient. We get,

$$\sum_p C_p^* C_q [H_{pq} + S_{pq} - EO_{pq}] = 0, \quad (4.13)$$

where

$$H_{pq} = \int_{I+II} \chi_p^* H \chi_q d\vec{r}, \quad (4.14)$$

$$O_{pq} = \int_{I+II} \chi_p^* \chi_q d\vec{r}, \quad (4.15)$$

and surface integral term is

$$S_{pq} = -\frac{1}{2} \int_{sphere} (\chi_p^{II} + \chi_p^I)^* \left(\frac{\partial}{\partial r} \chi_q^{II} - \frac{\partial}{\partial r} \chi_q^I \right) d\vec{s}, \quad (4.16)$$

where $d\vec{s}$ is surface element. The Energy E can take only those values for which the secular determinant is zero, i.e.

$$\det [H_{pq} + S_{pq} - EO_{pq}] = 0. \quad (4.17)$$

For a crystal with n atoms per unit cell, the matrix elements $M_{pq} = H_{pq} + S_{pq} - EO_{pq}$ for APW basis functions with wave vector $\vec{k}_p = \vec{k} + \vec{K}_p$ and $\vec{k}_q = \vec{k} + \vec{K}_q$, \vec{K}_p and \vec{K}_q are reciprocal lattice vectors index p and q , are given by

$$M_{pq} = (k_p^2 - E) \delta_{pq} - \frac{4\pi}{V} \sum_v^n e^{i(\vec{K}_p - \vec{K}_q) \cdot \vec{r}_v} R_v^2 \left[(\vec{k}_p \cdot \vec{k}_q - E) \frac{j_1 \left(\left| \vec{K}_p - \vec{K}_q \right| R_v \right)}{\left| \vec{K}_p - \vec{K}_q \right|} - \sum_{l=0}^{\infty} (2l+1) P_l \left(\vec{k}_p \cdot \vec{k}_q \right) j_l(k_p R_v) j_l(k_q R_v) \frac{u'_l(R_v)}{u_l(R_v)} \right], \quad (4.18)$$

where P_l are Legendre polynomial, $u_l(R_v)$ and $u'_l(R_v)$ is the radial functions and its radial derivative at the muffin tin radius R_v . To find the energy eigenvalues for a state with wave vector \vec{k} the matrix elements of M_{pq} are constructed and the determinant of this matrix is calculated on a fine energy grid where its determinant is zero. To avoid a very large basis set size, the APW basis determinant must therefore be re-evaluated for each new energy because it is non linear in

energy. In general, the search for APW eigenvalues becomes very time consuming as the determinant must be recalculated for a number of energies in order to localize the zero values as illustrated in Fig. 4.2.

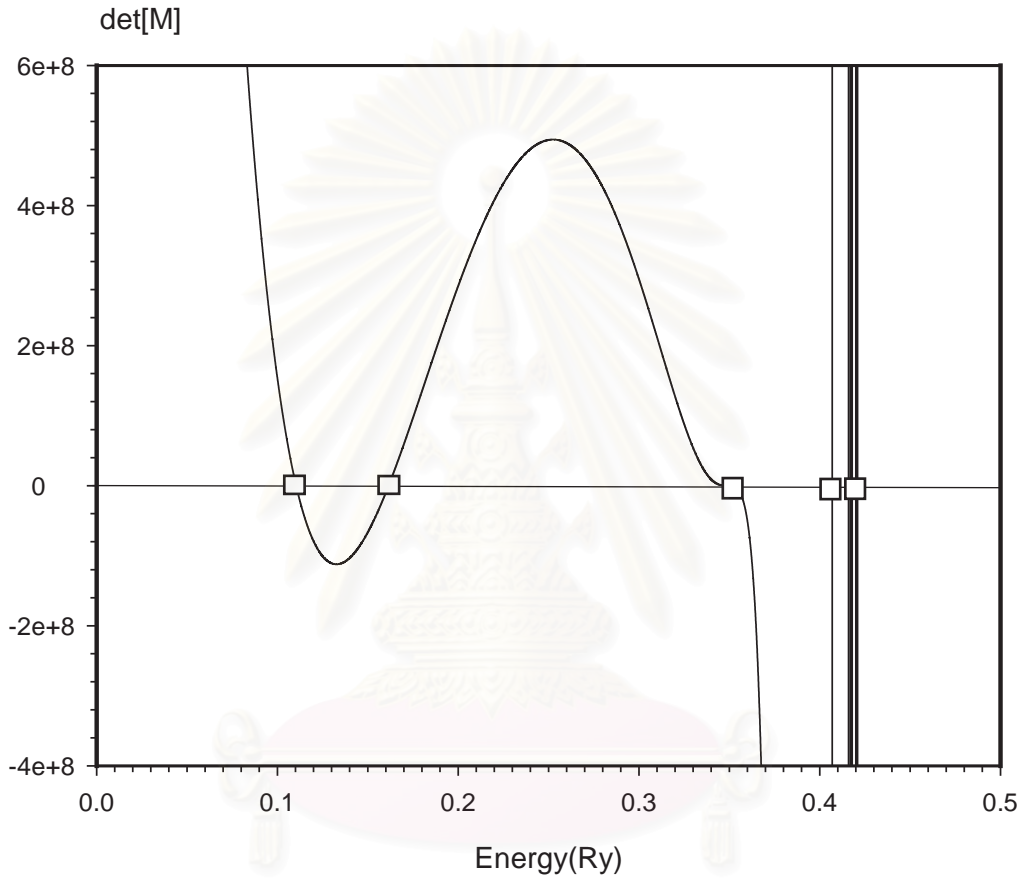


Fig. 4.2 The APW determinant of $H_{pq} + S_{pq} - EO_{pq}$ must be evaluated for a number of energies E . The square indicates the eigenenergies of the valence electrons in face-centered cubic copper at $k = \frac{2\pi}{a} (0.74, 0.74, 0.74)$ and $a = 6.822a_0$.

The task of finding the APW eigenvalues becomes somewhat more trouble when a large number of energies are involved, one might hit an energy in which

$u_l(R_v, E)$ is very small or even equal to zero. When it is inserted in the equation of coefficient, the coefficient is very large or infinite. The determinant involving matrix elements with summations over the coefficients, will go to infinite,

$$\det [H_{pq} + S_{pq} - EO_{pq}] \rightarrow \infty,$$

as

$$u_l(R_v, E) \rightarrow 0.$$

Therefore, the APW method is hardly used because of the energy dependent and an asymptotic problem. In next section, we shall describe the linearized augmented plane wave (LAPW) method which is based on the augmented plane wave but avoids the above problems.

4.3 The Linearized Augmented Plane Wave(LAPW)

An efficient way of avoiding the energy dependence problem in APW calculations would be to use a fixed energy E_p , called pivot, in which the basis functions are calculated with and to use these wave functions for a range of energies around the fixed energy. The idea of the LAPW[20-22] method is that the radial solutions of the basis set in the muffin tin sphere is approximated by an energy linearization[23-24]

$$u_l(r, E) = u_l(r, E_p) + (E - E_p) \dot{u}_l(r, E_p) + \dots, \quad (4.19)$$

where $\dot{u}_l(r, E_p)$ is a derivative of $u_l(r, E)$ with respect to energy at the E_p . In the remainder of this section, the dot stands for the energy derivative and the prime is used for the radial derivative for an arbitrary function $f(r, E)$

$$\dot{f}(r, E) = \frac{\partial}{\partial E} f(r, E), \quad (4.20)$$

and

$$f'(r, E) = \frac{\partial}{\partial r} f(r, E). \quad (4.21)$$

The energy derivative of the radial solution within the muffin tin is used in the radial solutions to match onto the plane wave outside the spheres. Note that the APW Hamiltonian depends only on energy via the radial solution, so if we take these solutions and their energy derivatives at a fixed energy into account, we have eliminated all energy dependence from the Hamiltonian. In comparison with the APW method, we have twice as many radial functions inside the muffin tin sphere, $u_l(r, E)$ and $\dot{u}_l(r, E)$, and we can match not only the value but also the derivative of the plane wave across the sphere boundary as shown in Fig. 4.3.

สถาบันวิทยบริการ
จุฬาลงกรณ์มหาวิทยาลัย

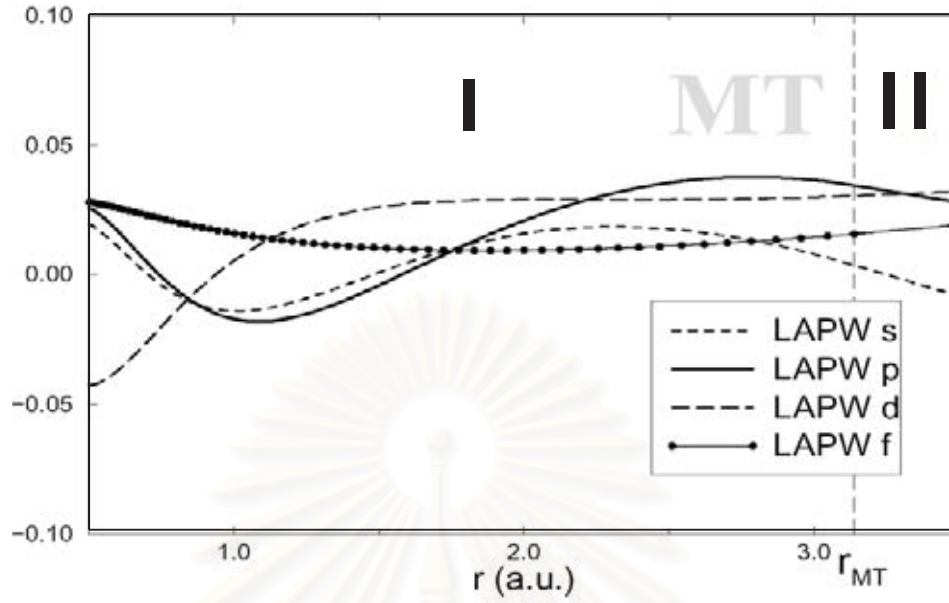


Fig 4.3 Parts of the radial l composition of a LAPW basis function for Cesium at the same \vec{k} point.

In summary, the LAPW function for the state which is specified by the wave vector \vec{k} , has the following form,

$$\begin{aligned} \chi_k^p(\vec{r}) &= \frac{1}{\sqrt{V}} e^{i(\vec{k} + \vec{K}_p) \cdot \vec{r}} = \frac{1}{\sqrt{V}} e^{i(\vec{k}_p) \cdot \vec{r}}, r \in II \\ &= \sum_{l=0}^{\infty} \sum_{m=-l}^l \{A_{lm}^p u_l(r, E_p) + B_{lm}^p \dot{u}_l(r, E_p)\}; r \in I \end{aligned} \quad (4.22)$$

where A_{lm} and B_{lm} are arbitrary constant and fixed by the matching conditions.

There is no energy dependence of the wave functions and the wave functions are smooth across the sphere boundary. However, the price to pay for this is to give up the exactness of the solution inside the sphere for the range of the pivot energies. From the equation of radial Schrödinger equation with energy E_l the

radial solutions must be normalized inside the muffin tin sphere

$$\int^{R_v} r^2 u_l^2(r, E) dr = 1, \quad (4.23)$$

and the energy derivative is obtained from the equation

$$-\frac{1}{r^2} \frac{d}{dr} \left(r^2 \frac{du_l(r, E)}{dr} \right) + \left[\frac{l(l+1)}{r^2} + U_v(r) \right] \dot{u}_l(r, E) - E \dot{u}_l(r, E) = u_l(r, E). \quad (4.24)$$

This is an inhomogeneous equation with $u_l(r, E)$ as its homogeneous solution.

Thus by obtaining a solution and orthogonalizing it to $u_l(r, E)$, we can obtain

$\dot{u}_l(r, E)$ and the normalization constant from the relation

$$R_v^2 [u'(R_v) \dot{u}(R_v) - u(R_v) \dot{u}'(R_v)] = 1. \quad (4.25)$$

Obviously, this is a different normalization from that applied to $u_l(r, E)$ since N_l

is given by

$$N_l = \int^{R_v} r^2 \dot{u}_l^2 dr. \quad (4.26)$$

This is generally not equal to unity. The expressions for the matrix elements are complicated. It depends on the normalizations for $u_l(r, E)$ and $\dot{u}_l(r, E)$ which will be specified below. The coefficients A_{lm} and B_{lm} obtained from the matching conditions are

$$A_{lm}^p = \frac{4\pi}{\sqrt{V}} R_v^2 i^l Y_m^{l*}(\hat{k}_p) a_l, \quad (4.27)$$

$$B_{lm}^p = \frac{4\pi}{\sqrt{V}} R_v^2 i^l Y_m^{l*}(\hat{k}_p) b_l, \quad (4.28)$$

where

$$a_l = j'_l(k_p R_v) \dot{u}_l(R_v) - j_l(k_p R_v) \dot{u}'_l(R_v), \quad (4.29)$$

and

$$b_l = j_l(k_p R_v) u'_l(R_v) - j'_l(k_p R_v) u_l(R_v). \quad (4.30)$$

The basis functions already satisfy the cellular boundary condition and connectivity conditions across the muffin tin spheres, so that, there is no surface integral. Thus, the variation yields a simple generalized eigenvalue problem with these energy independent overlap and Hamiltonian matrices. These matrices are reliable for some energy ranges around the pivot energy. It turns out that the resulting wave functions have inaccuracy of order $(E - E_p)^2$ as a result of the linearization and the energy eigenvalues deviate as order of $(E - E_p)^4$ from those evaluated at the correct energy. The matrix elements of the overlap matrix and the Hamiltonian can be calculated. The results are

$$O_{pq} = U(\vec{k}_p - \vec{k}_q) + \sum_v^n e^{i|\vec{K}_p - \vec{K}_q| \cdot \vec{\tau}_v} \frac{4\pi R_v^4}{V} \sum_{l=0} (2l+1) P_l(\hat{k}_p \cdot \hat{k}_q) s_{pq}^l, \quad (4.31)$$

where $U(\vec{k}_p - \vec{k}_q)$ is Fourier transform of the step function which is zero inside the muffin tin spheres and one outside,

$$U(\vec{k}_p - \vec{k}_q) = \delta_{\vec{k}_p, \vec{k}_q} - \sum_v^n e^{i|\vec{K}_p - \vec{K}_q| \cdot \vec{\tau}_v} \frac{4\pi R_v^2}{V} \frac{j_1\left(\left|\vec{K}_p - \vec{K}_q\right| R_v\right)}{\left|\vec{K}_p - \vec{K}_q\right|}, \quad (4.32)$$

where

$$s_{pq}^l = a_l(k_q) a_l(k_p) + b_l(k_q) b_l(k_p) N_l, \quad (4.33)$$

and $P_l(\hat{k}_p \cdot \hat{k}_q)$ is the Legendre polynomial. Similarly, the Hamiltonian matrix is obtained as

$$H_{pq} = (\vec{k}_p \cdot \vec{k}_q) U(\vec{k}_p - \vec{k}_q) + \sum_v^n e^{i\vec{k}_n \cdot \vec{\tau}_v} \frac{4\pi R_v^4}{\Omega} (2l + 1) P_l(\hat{k}_p \cdot \hat{k}_q) (E_l s_{pq}^l + \gamma^l), \quad (4.34)$$

where

$$\begin{aligned} \gamma^l = & \dot{u}_l(R_v) u'_l(R_v) [j'_l(k_q) j'_l(k_p) + j_l(k_q) j_l(k_p)] \\ & - [\dot{u}'_l(R_v) u'_l(R_v) j_l(k_q) j_l(k_p) + \dot{u}_l(R_v) u_l(R_v) j'_l(k_q) j'_l(k_p)]. \end{aligned} \quad (4.35)$$

This is explicitly Hermitian and it is the actual form that we use in our code. Another quantity of interest is the charge density which is needed for calculating the the Hartree and exchange-correlation potentials in the density functional theory self-consistency loop.

4.4 Brillouin Zone Integration

Many calculations of crystals involve the integration of a periodic functions of Bloch wave vector over either the entire Brillouin zone or over specified portions. The latter case arises, for example, in averages over states within the Fermi surface. The accuracy and the computational effort of the electronic structure calculations for solids depend directly on these Brillouin zone integrations, because they determine how many k points that we must consider for a given ac-

curacy. Thus, this section presents the tetrahedron method which is a Brillouin zone integration method.

For the Brillouin zone integrations, the following two methods are most widely used, i.e. the tetrahedron method[25-26] and the special point scheme[27-29]. The special point scheme, which is limited to insulating or semiconducting materials, represents the Brillouin Zone integration as a weighted sum over selected k points. A more general integration scheme is the tetrahedron method which is equally applicable to insulators and metals. In this method, the reciprocal space is divided into several tetrahedra in which matrix elements and band energies are linearized in k . The linear approximation allows the integration to be performed analytically. It takes into account the complicated shape of the Fermi surface. In addition, the tetrahedron method is superior to the special point method because it gives spectral functions.

Before the presentation of the tetrahedron method, we would like to introduce first the Brillouin zone for some specific structures.

4.4.1 The Body-Centered Cubic Lattice.

The primitive translation vectors (a_1, a_2, a_3) of the body-centered cubic lattice are

$$\begin{aligned}\vec{a}_1 &= \frac{a}{2}(-\hat{x} + \hat{y} + \hat{z}), \\ \vec{a}_2 &= \frac{a}{2}(\hat{x} - \hat{y} + \hat{z}),\end{aligned}\tag{4.36}$$

$$\vec{a}_3 = \frac{a}{2} (\hat{x} + \hat{y} - \hat{z}),$$

where a is lattice constant, $\hat{x}, \hat{y}, \hat{z}$ are unit vectors in x,y,z directions respectively and the volume of the primitive cell is

$$V = |\vec{a}_1 \cdot \vec{a}_2 \times \vec{a}_3| = \frac{a^3}{2}.$$

We obtain the reciprocal lattice vectors (b_1, b_2, b_3) as

$$\begin{aligned} \vec{b}_1 &= \frac{2\pi}{a} (\hat{y} + \hat{z}), \\ \vec{b}_2 &= \frac{2\pi}{a} (\hat{x} + \hat{z}), \\ \vec{b}_3 &= \frac{2\pi}{a} (\hat{x} + \hat{y}), \end{aligned} \tag{4.37}$$

and the general reciprocal lattice vector \vec{K} is, for integer n_1, n_2 and n_3 , is

$$\vec{K} = \frac{2\pi}{a} [(n_2 + n_3) \hat{x} + (n_1 + n_3) \hat{y} + (n_1 + n_2) \hat{z}]. \tag{4.38}$$

The first Brillouin zone is thus the rhombododecahedron, shown in Fig.4.4.

4.4.2 The Face-Centered Cubic Lattice.

The primitive translation vectors (a_1, a_2, a_3) of the body-centered cubic lattice are

$$\begin{aligned} \vec{a}_1 &= \frac{a}{2} (\hat{y} + \hat{z}), \\ \vec{a}_2 &= \frac{a}{2} (\hat{x} + \hat{z}), \\ \vec{a}_3 &= \frac{a}{2} (\hat{x} + \hat{y}), \end{aligned} \tag{4.39}$$

and the volume of the primitive cell is

$$V = |\vec{a}_1 \cdot \vec{a}_2 \times \vec{a}_3| = \frac{a^3}{4}.$$

We obtain the reciprocal lattice vectors (b_1, b_2, b_3) as

$$\begin{aligned}\vec{b}_1 &= \frac{2\pi}{a} (-\hat{x} + \hat{y} + \hat{z}), \\ \vec{b}_2 &= \frac{2\pi}{a} (\hat{x} - \hat{y} + \hat{z}), \\ \vec{b}_3 &= \frac{2\pi}{a} (\hat{x} + \hat{y} - \hat{z}),\end{aligned}\tag{4.40}$$

and the general reciprocal lattice vector \vec{K} is, for integer n_1, n_2 and n_3 , is

$$\vec{K} = \frac{2\pi}{a} [(-n_1 + n_2 + n_3)\hat{x} + (n_1 - n_2 + n_3)\hat{y} + (n_1 + n_2 - n_3)\hat{z}].\tag{4.41}$$

The first Brillouin zone is the truncated octahedron shown in Fig.4.4.

4.4.3 The Hexagonal Close-Packed Lattice.

The primitive translation vectors (a_1, a_2, a_3) of the body centered cubic lattice are

$$\begin{aligned}\vec{a}_1 &= c\hat{z}, \\ \vec{a}_2 &= a\hat{x}, \\ \vec{a}_3 &= a\left(\frac{\hat{x}}{2} + \frac{\sqrt{3}}{2}\hat{y}\right),\end{aligned}\tag{4.42}$$

where a and c is a lattice constant in the xy plane and z direction respectively, and the volume of the primitive cell is

$$\Omega = |\vec{a}_1 \cdot \vec{a}_2 \times \vec{a}_3| = \frac{\sqrt{3}}{2}a^2c.$$

We obtain the reciprocal lattice vectors (b_1, b_2, b_3) as

$$\begin{aligned}\vec{b}_1 &= \frac{2\pi}{c}\hat{z}, \\ \vec{b}_2 &= \frac{2\pi}{a}\hat{x} + \frac{2\pi}{a\sqrt{3}}\hat{y}, \\ \vec{b}_3 &= \frac{2\pi}{a}\frac{2}{\sqrt{3}}\hat{y},\end{aligned}\tag{4.43}$$

and the general reciprocal lattice vector \vec{K} is, for integer n_1, n_2 and n_3 , is

$$\vec{K} = \frac{2\pi}{a} \left[n_2\hat{x} + \left(n_2\frac{1}{\sqrt{3}} + n_3\frac{2}{\sqrt{3}} \right) \hat{y} + \frac{a}{c}n_1\hat{z} \right].\tag{4.44}$$

The first Brillouin zone is shown in Fig.4.4.

สถาบันวิทยบริการ
จุฬาลงกรณ์มหาวิทยาลัย

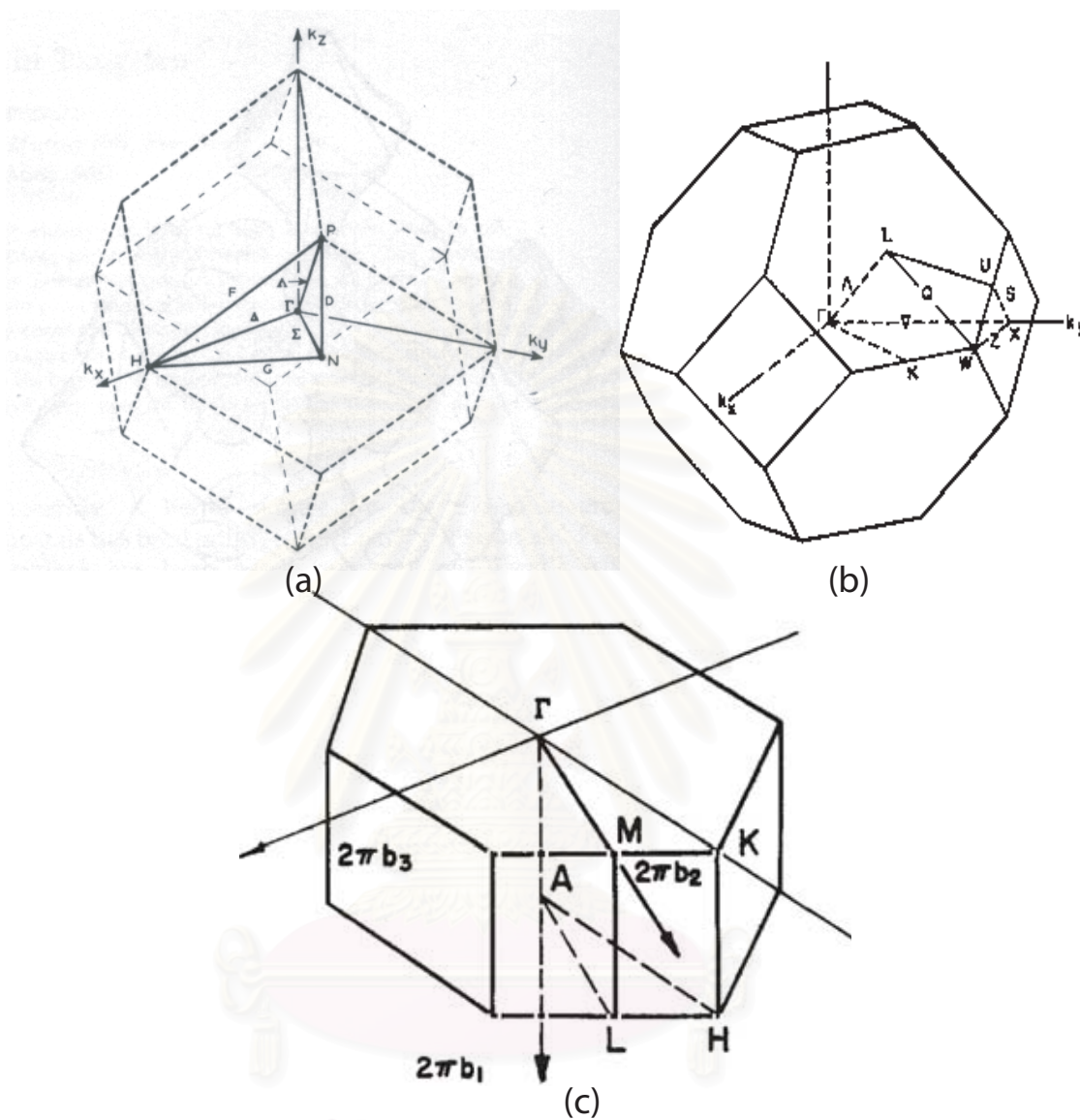


Fig. 4.4 The fundamental domain of k or first Brillouin zone for (a) the body-centered cubic lattice (b) the face-centered cubic lattice and (c) the hexagonal close-packed lattice.

4.4.4 The Tetrahedron Method

In a crystalline solid, the lattice translation symmetry results in a quantum number. The wave function $\psi_n(\vec{k})$ and the eigenvalue $E_n(\vec{k})$ depend on the band index n and the crystal momentum \vec{k} . The expectation value $\langle A \rangle$ of an operator A is obtained by integrating the matrix elements $A_n(\vec{k})$ over occupied states in reciprocal space as

$$\langle A \rangle = \frac{1}{V_G} \sum_n \int_{V_G} A_n(\vec{k}) f(E_n(\vec{k})) d^3k, \quad (4.45)$$

where $A_n(\vec{k}) = \langle \psi_n(\vec{k}) | A | \psi_n(\vec{k}) \rangle$. V_G is the volume of the reciprocal unit cell and $f(E_n(\vec{k}))$ is the occupation number. In this work, we consider only the Fermi distribution function at absolute zero. It is equal to 1 for $E < E_F$ and zero for $E > E_F$. For metals, the tetrahedron method can be expressed so that the expectation value $\langle A \rangle$ of an operator A is obtained by changing integral to sum over irreducible \vec{k} points

$$\langle A \rangle = \sum_{j,n} A_n(\vec{k}_j) w_{n,j}, \quad (4.46)$$

where $w_{n,j}$ are called weight and are obtained in the next. These weight are independent of the matrix elements $A_n(\vec{k})$ and they are calculated only once for a given set of energy bands with the tetrahedron method.

Firstly, we define an equispaced grid in the reciprocal space. The lattice vectors of the submesh are obtained by dividing a set of the primitive reciprocal

lattice vectors by integer m_1, m_2 and m_3 . Each submesh cell is divided into six tetrahedra. As illustrated in Fig 4.5, we choose one main diagonal of a submesh cell as a common edge of all six tetrahedra.

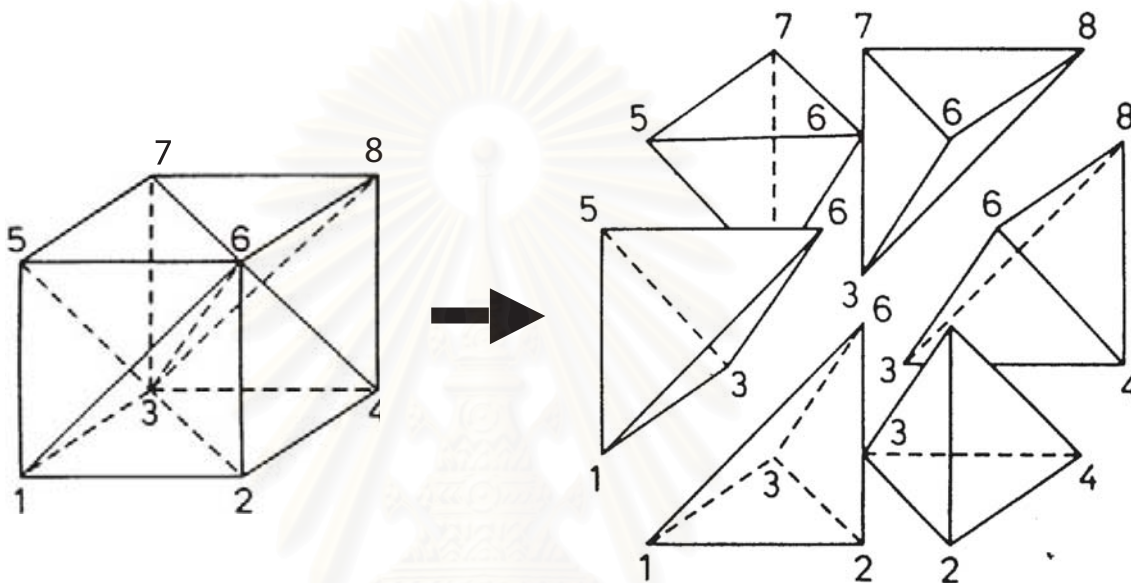


Fig. 4.5 Break up of a submesh cell into six tetrahedra.

In order to minimize interpolation distances, the shortest main diagonal is chosen. The energy $E(\vec{k})$ is linearly expanded inside the tetrahedron and the coefficients of expansion are determined in term of the corner energies and the coordinates of wave vector \vec{k} . For this purpose it is convenient to arrange the energy at the corner of the tetrahedrons in an increasing or a decreasing order. Let \vec{k}_i ($i = 1, 2, 3, 4$) be the coordinates of the four corners of the tetrahedron with associated and E_i . we assume $E_1 < E_2 < E_3 < E_4$. The density of states $D(E)$

and the number of states $n(E)$ or the integrated density of states from a given tetrahedron are

$$D(E) = 0, \quad (4.47)$$

$$n(E) = 0. \quad (4.48)$$

For $E < E_1$,

$$D(E) = \frac{V_T 3(E - E_1)^2}{V_G E_{21} E_{31} E_{41}}, \quad (4.49)$$

$$n(E) = \frac{V_T (E - E_1)^3}{V_G E_{21} E_{31} E_{41}}, \quad (4.50)$$

for $E_1 < E < E_2$,

$$D(E) = \frac{V_T}{V_G E_{31} E_{41}} \left[3E_{21} + 6(E - E_2) - 3 \frac{E_{31} + E_{42}}{E_{32} E_{42}} (E - E_2)^2 \right], \quad (4.51)$$

$$n(E) = \frac{V_T}{V_G E_{31} E_{41}} \left[E_{21}^2 + 3E_{21}(E - E_2) + 3(E - E_2)^2 - \frac{E_{31} + E_{42}}{E_{32} E_{42}} (E - E_2)^3 \right], \quad (4.52)$$

for $E_2 < E < E_3$,

$$D(E) = \frac{V_T 3(E - E_2)^2}{V_G E_{41} E_{42} E_{43}}, \quad (4.53)$$

$$n(E) = \frac{V_T}{V_G} \left(1 - \frac{(E - E_2)^3}{E_{41} E_{42} E_{43}} \right), \quad (4.54)$$

for $E_3 < E < E_4$, and

$$D(E) = 0, \quad (4.55)$$

$$n(E) = \frac{V_T}{V_G}, \quad (4.56)$$

for $E > E_4$, where E_{ij} is a shorthand notation for $E_i - E_j$ and V_T is the reciprocal space volume of the tetrahedron. Note that, the band index n is suppressed. After a number of states is calculated, it is used to determine the Fermi energy level. The weight is also evaluated by using these expressions. For a fully unoccupied tetrahedron, $E_F < E_1$, the contributions vanish, i.e.

$$w_1 = w_2 = w_3 = w_4 = 0. \quad (4.57)$$

For $E_1 < E_F < E_2$,

$$w_1 = C \left[4 - (E_F - E_1) \left(\frac{1}{E_{21}} + \frac{1}{E_{31}} + \frac{1}{E_{41}} \right) \right], \quad (4.58)$$

$$w_2 = C \frac{(E_F - E_1)}{E_{21}}, \quad (4.59)$$

$$w_3 = C \frac{(E_F - E_1)}{E_{31}}, \quad (4.60)$$

$$w_4 = C \frac{(E_F - E_1)}{E_{41}}, \quad (4.61)$$

with

$$C = \frac{V_T (E_F - E_1)^3}{4V_G E_{21} E_{31} E_{41}}.$$

For $E_2 < E_F < E_3$,

$$w_1 = C_1 + (C_1 + C_2) \frac{(E_3 - E_F)}{E_{31}} + (C_1 + C_2 + C_3) \frac{E_4 - E_F}{E_{41}}, \quad (4.62)$$

$$w_2 = C_1 + C_2 + C_3 + (C_2 + C_3) \frac{E_3 - E_F}{E_{32}} + C_3 \frac{E_4 - E_F}{E_{42}}, \quad (4.63)$$

$$w_3 = (C_1 + C_2) \frac{E_F - E_1}{E_{31}} + (C_2 + C_3) \frac{E_F - E_2}{E_{32}}, \quad (4.64)$$

$$w_4 = (C_1 + C_2 + C_3) \frac{E_F - E_1}{E_{41}} + C_3 \frac{E_F - E_2}{E_{42}}, \quad (4.65)$$

with

$$C_1 = \frac{V_T}{4V_G} \frac{(E_F - E_1)^2}{E_{31}E_{41}},$$

$$C_2 = \frac{V_T}{4V_G} \frac{(E_F - E_1)(E_F - E_2)(E_3 - E_F)}{E_{31}E_{31}E_{41}},$$

$$C_3 = \frac{V_T}{4V_G} \frac{(E_F - E_2)^2(E_4 - E_F)}{E_{41}E_{32}E_{42}}.$$

For $E_3 < E_F < E_4$,

$$w_1 = \frac{V_T}{4V_G} - C \frac{(E_4 - E_F)}{E_{41}}, \quad (4.66)$$

$$w_2 = \frac{V_T}{4V_G} - C \frac{(E_4 - E_F)}{E_{42}}, \quad (4.67)$$

$$w_3 = \frac{V_T}{4V_G} - C \frac{(E_4 - E_F)}{E_{43}}, \quad (4.68)$$

$$w_4 = \frac{V_T}{4V_G} - C \left[4 - (E_4 - E_F) \left(\frac{1}{E_{43}} + \frac{1}{E_{42}} + \frac{1}{E_{41}} \right) \right], \quad (4.69)$$

with

$$C = \frac{V_T}{4V_G} \frac{(E_4 - E_F)^3}{E_{43}E_{42}E_{41}}.$$

For a fully occupied tetrahedron the contribution for each corners is identical, i.e.

$$w_1 = w_2 = w_3 = w_4 = \frac{V_T}{4V_G}. \quad (4.70)$$

The correction terms of the weight factors have a simple form

$$dw_i = \sum_T \frac{1}{40} D_T(E_F) \sum_{j=1}^4 (E_j - E_i). \quad (4.71)$$

where $D_T(E_F)$ is the density of state of the T^{th} tetrahedra at the Fermi energy. In a finite Temperature case, the step function is replaced by the Fermi distribution and the Fermi energy is determined from the requirement that

$$N = \sum_k \sum_n w(k, \epsilon_n(k) - E_F), \quad (4.72)$$

where the weights are given by

$$w(k, \epsilon_n(k) - E_F) = w(k) \frac{1}{e^{(\epsilon_n(k) - E_F)/k_B T} + 1}. \quad (4.73)$$

4.5 The Full Potential Linearized Augmented Plane Wave(FP-LAPW)

In full potential augmented plane wave method[30-32], there is no shape approximation of the potential and the density in the interstitial and inside the muffin tin region. The potential is expanded in the following form

$$\begin{aligned} V(\vec{r}) &= \sum_K V_K e^{i\vec{K}\cdot\vec{r}}; r \in II \\ &= \sum_{l=0}^{\infty} \sum_{m=-l}^l V_{lm}(r) Y_{lm}(\hat{r}); r \in I, \end{aligned} \quad (4.74)$$

where V_K is the Fourier coefficient of the potential $V(\vec{r})$ and $V_{lm}(r)$ is a spherical harmonic coefficient which is the projection of the potential $V(\vec{r})$ onto the harmonic coefficient $Y_{lm}(\hat{r})$. The muffin tin approximation used in early calculations corresponds to containing in Eq.(4.74) only the $K = 0$ component in the

first expression and only the $l = 0$ and $m = 0$ components in the second. Again, the charge density $|\Psi|^2$ is represented in the same way as the potential

$$\begin{aligned}
 n(\vec{r}) &= \sum_{\vec{k},n} \left| \psi_{\vec{k},n}(\vec{r}) \right|^2 w(k,n) \\
 &= \sum_K n_K e^{i\vec{K}\cdot\vec{r}}; r \in II \\
 &= \sum_{l=0}^{\infty} \sum_{m=-l}^l n_{lm}(r) Y_{lm}(\hat{r}); r \in I, \tag{4.75}
 \end{aligned}$$

where n_K is the Fourier coefficient of the density $n(\vec{r})$ and $n_{lm}(r)$ is a spherical harmonic coefficient which is the projection of the density $n(\vec{r})$ onto the harmonic coefficient $Y_{lm}(\hat{r})$. The plane wave coefficients of the electron density are

$$n_K = \frac{1}{V} \sum_{k,n} \sum_{K',K'',K''-K'=K} \left(C_n^{K'}(k) \right)^* C_n^{K''}(k) w(k,n), \tag{4.76}$$

where $C_n^K(k)$ is the coefficient which is the projection of the wave function $\psi_{kn}(\vec{r})$ onto the basis vectors $\chi_k^K(\vec{r})$. and the density spherical harmonic coefficients n_{lm} are[33]

$$\begin{aligned}
 n_{l''m''} &= \sum_{l,l} \left(\sum_k \sum_n \sum_{m',m} (A_{l'm',n}(k))^* A_{lm,n}(k) G_{ll''}^{mm'm''} w(n,k) \right) u_{l'}(r) u_l(r) \\
 &+ \sum_{l,l} \left(\sum_k \sum_n \sum_{m',m} (A_{l'm',n}(k))^* B_{lm,n}(k) G_{ll''}^{mm'm''} w(n,k) \right) u_{l'}(r) \dot{u}_l(r) \\
 &+ \sum_{l,l} \left(\sum_k \sum_n \sum_{m',m} (B_{l'm',n}(k))^* A_{lm,n}(k) G_{ll''}^{mm'm''} w(n,k) \right) \dot{u}_{l'}(r) u_l(r) \\
 &+ \sum_{l,l} \left(\sum_k \sum_n \sum_{m',m} (B_{l'm',n}(k))^* B_{lm,n}(k) G_{ll''}^{mm'm''} w(n,k) \right) \\
 &\cdot (\dot{u}_{l'}(r) \dot{u}_l(r)), \tag{4.77}
 \end{aligned}$$

with

$$\begin{aligned}
 G_{l'l''}^{mm'm''} &= \int Y_{lm}^* Y_{l'm'} Y_{l''m''} d\Omega = \int Y_{lm} Y_{l'm'}^* Y_{l''m''}^* d\Omega \\
 &= \left[\frac{(2l'+1)(2l''+1)}{4\pi(2l+1)} \right]^{\frac{1}{2}} \\
 &\quad \cdot [C(l', l'', l : m', m'', m) C(l', l'', l : 0, 0, 0)], \quad (4.78)
 \end{aligned}$$

where $C(l', l'', l : m', m'', m)$ is Clebsh-Gordan coefficient and

$$\begin{aligned}
 A_{lm,n}(k) &= \sum_K C_n^K(k) A_{lm}^K(k), \\
 B_{lm,n}(k) &= \sum_K C_n^K(k) B_{lm}^K(k). \quad (4.79)
 \end{aligned}$$

4.5.1 Construction of the Full Potential

The Coulomb potential V_c consists of two parts: Hartree potential $V_H(\vec{r})$ and potential of nuclei. The Hartree-potential is determined from the charge density via the poisson equation

$$\nabla^2 V_H(\vec{r}) = -8\pi n(\vec{r}), \quad (4.80)$$

where $n(\vec{r})$ is the density. Solving this equation with plane wave basis is not so difficult, as the Laplace operator is diagonal in the reciprocal space. For the muffin tin region, the pseudocharge method developed by Weinert[34] is used to calculate the Hartree-potential without the shape approximation. The method is based on the concept of multipole potentials and the spherical boundary value problem. It has two steps. In the first step, the true muffin tin charge is replaced by a

pseudocharge density, $\tilde{n}(\vec{r})$, that leads to the same potential outside the muffin tin. The interstitial potential is calculated in the reciprocal space

$$V_I(\vec{r}) = \sum_{K \neq 0} \frac{8\pi\tilde{n}_K}{K^2} e^{i\vec{K}\cdot\vec{r}}, \quad (4.81)$$

where \tilde{n}_K is Fourier of pseudocharge density.

In the second step, the muffin tin potential is determined from the Dirichlet boundary value problem which is defined by the exact muffin tin charge and the interstitial potential on the muffin tin sphere boundaries, i.e.

$$V(\vec{r}) = \int_S n(\vec{r}_1) G(\vec{r}, \vec{r}_1) d^3\vec{r}_1 - \frac{R_v^2}{4\pi} \oint_S V_I(R_{1v}) \left(\frac{\partial G}{\partial r_1} \right)_{R_v} d\Omega_1, \quad (4.82)$$

where R_v is a point on the sphere and the Green's function $G(\vec{r}, \vec{r}_1)$ is given by

$$G(\vec{r}, \vec{r}_1) = 4\pi \sum_{lm} \frac{Y_{lm}^*(\hat{r}_1) Y_{lm}(\hat{r})}{2l+1} \frac{r_{<}^l}{r_{>}^{l+1}} \left[1 - \left(\frac{r_{>}}{R} \right)^{2l+1} \right], \quad (4.83)$$

where $r_{>}(r_{<})$ is the greater (smaller) of r and r_1 , the normal derivative is

$$\left(\frac{\partial G}{\partial r_1} \right)_v = -\frac{4\pi}{R_v^2} \sum_{lm} \left(\frac{r}{R_v} \right)^l Y_{lm}^*(\hat{r}_1) Y_{lm}(\hat{r}), \quad (4.84)$$

We synthesize the spherical harmonic components of V_K on the sphere and use the Green's function to compute the potential $V_{lm}(r)$ within the sphere. It can

be written as

$$\begin{aligned}
V_{lm}(r) = & (4\pi)^2 \sum_{K \neq 0} \sum_v e^{i\vec{K} \cdot \vec{\tau}_v} \frac{2\tilde{n}_K}{K^2} i^l j_l(KR) R^2 Y_{lm}^*(\hat{K}) Y_{lm}(\hat{r}) \left(\frac{r}{R}\right)^l \\
& + \frac{4\pi}{2l+1} \left[\frac{1}{r^{l+1}} \int_0^r 2n_{lm}(r') (r')^{l+2} dr' - \frac{2}{\sqrt{4\pi}} \left[\frac{1}{r}\right] \delta_{l0} \right] \\
& + \frac{4\pi}{2l+1} \left[-\frac{r^l}{R^{2l+1}} \int_0^R 2n_{lm}(r') (r')^{l+2} dr' \right] \\
& + \frac{4\pi}{2l+1} \left[r^l \int_r^R 2n_{lm}(r') (r')^{1-l} dr' \right]. \tag{4.85}
\end{aligned}$$

where δ_{l0} is a Kronecker delta $l, 0$. Finally, the muffin tin potential has to be expanded into spherical harmonics and the potential of the nuclei is added to the spherical ($l = 0$) component of the effective potential.

The problem of the determination of the exchange-correlation potential V_{xc} is different from the Coulomb potential because the exchange-correlation contribution depends only on the position \vec{r} . The calculation of the exchange potential in the muffin tin has two steps. In the first step, the charge density is calculated on a set of the real space. In the second step, the exchange potential is calculated and expanded in spherical harmonics of which coefficients can be obtained from

$$v_{xc,lm}(r) = \int Y_{lm}^*(\hat{r}) V_{xc}(\vec{r}) d\Omega. \tag{4.86}$$

where $v_{xc,lm}(r)$ is a spherical harmonic coefficient which is the projection of the exchange-correlation potential $V_{xc}(\vec{r})$ onto the harmonic coefficient $Y_{lm}(\hat{r})$. In the

interstitial region, The three-dimensional fast Fourier is used because the charge density is expanded into three dimensional plane waves. Again, the exchange potential is calculated on the real space. Finally $V_{xc,K}$, which is the Fourier coefficient of the exchange-correlation potential $V_{xc}(\vec{r})$, is the reverse transformed.

4.5.2 Construction of the Full Hamiltonian

To include the full potential or non muffin effect, the Hamiltonian matrix is modified. It has the following form

$$\begin{aligned}
H_{pq} = & \left(\vec{k}_p \cdot \vec{k}_q \right) U \left(\vec{k}_p - \vec{k}_q \right) + \sum_{K'} V_{K'} U \left(\vec{K}' + \vec{k}_p - \vec{k}_q \right) + \\
& \sum_v e^{i(\vec{K}_q - \vec{K}_p) \cdot \vec{\tau}_v} \frac{4\pi R_v^4}{\Omega} (2l + 1) P_l \left(\hat{k}_p \cdot \hat{k}_q \right) \left(E_l s_{pq}^l + \gamma^l \right) \\
& + \sum_v e^{i(\vec{K}_q - \vec{K}_p) \cdot \vec{\tau}_v} \sum_{lm, l' m'} \sum_{L=1, M} G_{ll'}^{mMm'} \cdot \\
& \left[\int_0^{R_v} dr r^2 \left(A_{l'm'}^p(k_p) u_{l'} + B_{l'm'}^p(k_p) \dot{u}_{l'} \right)^* V_{LM} \right. \\
& \left. \left(A_{lm}^q(k_q) u_l + B_{lm}^q(k_q) \dot{u}_l \right) \right]. \tag{4.87}
\end{aligned}$$

where $G_{ll'}^{mMm'}$ is defined in Eq.(4.78) and A_{lm}^q , B_{lm}^q are defined in Eq.(4.27-4.28).

In order to minimize the linearization error, the energy parameters should be chosen as close to the band energies as possible. However, the band energies $\epsilon_n(k)$ depend on \vec{k} whereas the energy parameters are constants. In addition, the radial functions contribute to the eigenfunctions of the different bands with different energies. An optimal choice can be obtained from the requirement that

the energy parameters minimize

$$\sum_k \sum_n (\epsilon_n(k) - E_l)^2 n_{n,l}(k) w(k, n). \quad (4.88)$$

where

$$n_{n,l}(k) = \sum_{m=-l}^l |A_{lm,n}(k)|^2 + |B_{lm,n}(k)|^2 N_l. \quad (4.89)$$

By setting the derivative $\left(\frac{\partial}{\partial E_l}\right)$ of Eq.(4.88) equal to zero, it yields the optimal energy parameter

$$E_l = \frac{\sum_k \sum_n \epsilon_n(k) n_{n,l}(k) w(k, n)}{\sum_k \sum_n n_{n,l}(k) w(k, n)}, \quad (4.90)$$

4.5.3 Mixing Scheme

The aim of the electronic structure calculations is to minimize the energy functional with respect to the electron density. The minimization of the density functional is performed implicitly by the self-consistent density. The construction of new density from the resulting single particle wave functions is described as

$$n^{new}(\vec{r}) = F \{n^{old}(\vec{r})\}. \quad (4.91)$$

This scheme is in general divergent. Thus it is necessary to stabilize the self-consistent cycle by mixing the new density with the old (input) density to obtain the density actually used in the next iteration as

$$n^{new}(\vec{r}) = (1 - \alpha)n^{old}(\vec{r}) + \alpha F \{n^{old}(\vec{r})\},$$

where α is between 0 and 1. In this work, we find that $\alpha = 0.3$ is the most optimum choice.

4.5.4 Total Energy Calculation

From the density functional theory, a simple expression for the total energy per unit cell is

$$E = \sum_{kn} \epsilon_n(k) w_{kn} - \frac{1}{2} \int_{\Omega} 2n(\vec{r}) [V_c(\vec{r}) + 2V_{xc}(\vec{r})] d\vec{r} - \frac{1}{2} \sum_v Z_v V_M(\vec{r}_v) + E_{xc}[n(\vec{r})], \quad (4.92)$$

where $\epsilon_n(k)$ is the dispersion relation, $n(\vec{r})$ is the density, $V_{xc}(\vec{r})$ and $E_{xc}[n(\vec{r})]$ is the exchange-correlation potential and exchange-correlation energy. $V_c(\vec{r})$ is the Coulomb potential. $V_M(\vec{r}_v)$ is a generalized Madelung potential[20] which is the Coulomb potential at the positions \vec{r}_v of nuclei due to all charges in the crystal except own the nuclear charge. The Madelung potential of hydrogen is defined as

$$V_M(\vec{r}_v) = \int \frac{2n(\vec{r}) d\vec{r}}{|\vec{r} - \vec{r}_v|} - \sum_{\alpha} \frac{2Z_{\alpha}}{|\vec{R}_{\alpha} - \vec{r}_v|}. \quad (4.93)$$

Again, the solution of poisson's equation of Madelung potential is solved by the pseudocharge method. The solution is

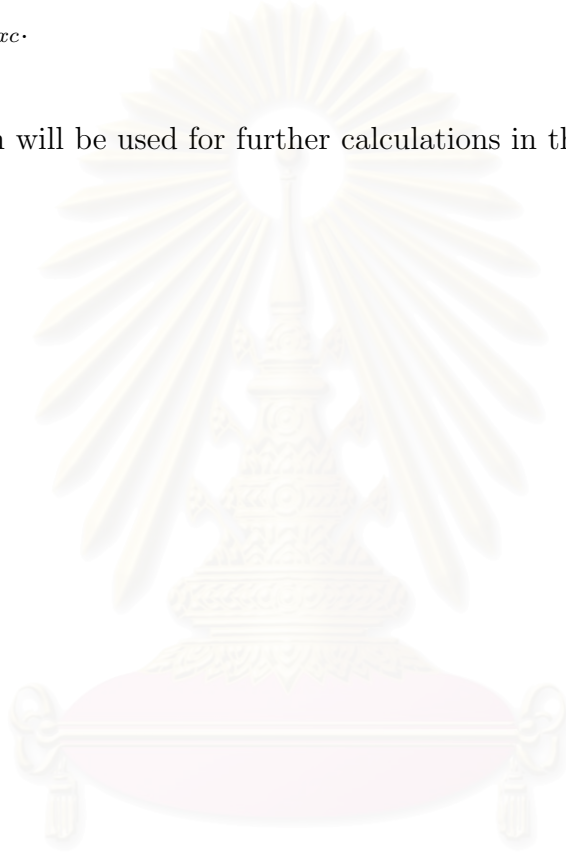
$$V_M(\vec{r}_v) = \frac{1}{R_v} [R_v S_0(R_v) + 2Z_v - 2Q_v] + 2\sqrt{4\pi} \int_0^{R_v} dr r n_{00}(r), \quad (4.94)$$

where $S_0(R_v)$ is the spherical average of the coulomb potential about centered R_v and Q_v is the total electronic charge in the sphere, $n_{00}(r)$ is a spherical harmonic

coefficient with $l, m = 0$. Then, the simplifying total energy is

$$\begin{aligned}
 E = & \sum_{kn} \epsilon_n(k) w_{kn} - \frac{1}{2} \left[\int_V 2n(\vec{r}) V_c(\vec{r}) d\vec{r} + 2\sqrt{4\pi} \sum_v Z_v \int_0^{R_v} dr r n_{00}(r) \right] \\
 & - \int_V 2n(\vec{r}) V_{xc}(\vec{r}) d\vec{r} - \frac{1}{2} \sum_v \frac{1}{R_v} [R_v S_0(R_v) + 2Z_v - 2Q_v] \\
 & + E_{xc}.
 \end{aligned} \tag{4.95}$$

This expression will be used for further calculations in the next chapter.



สถาบันวิทยบริการ
จุฬาลงกรณ์มหาวิทยาลัย

Chapter 5

Calculation of the Ground State Energy

5.1 Introduction

In this chapter, we calculate the ground state energy of the solid metallic hydrogen by using the two methods, Wigner-Seitz method and FP-LAPW, described in previous chapters. In addition, the energy bands and the density of states are calculated by FP-LAPW.

5.2 The Total Ground State Energy of the Solid Metallic Hydrogen by the Wigner-Seitz Method

From Eq. (3.31), the ground state energy of the solid metallic hydrogen as a function of r_s is calculated.

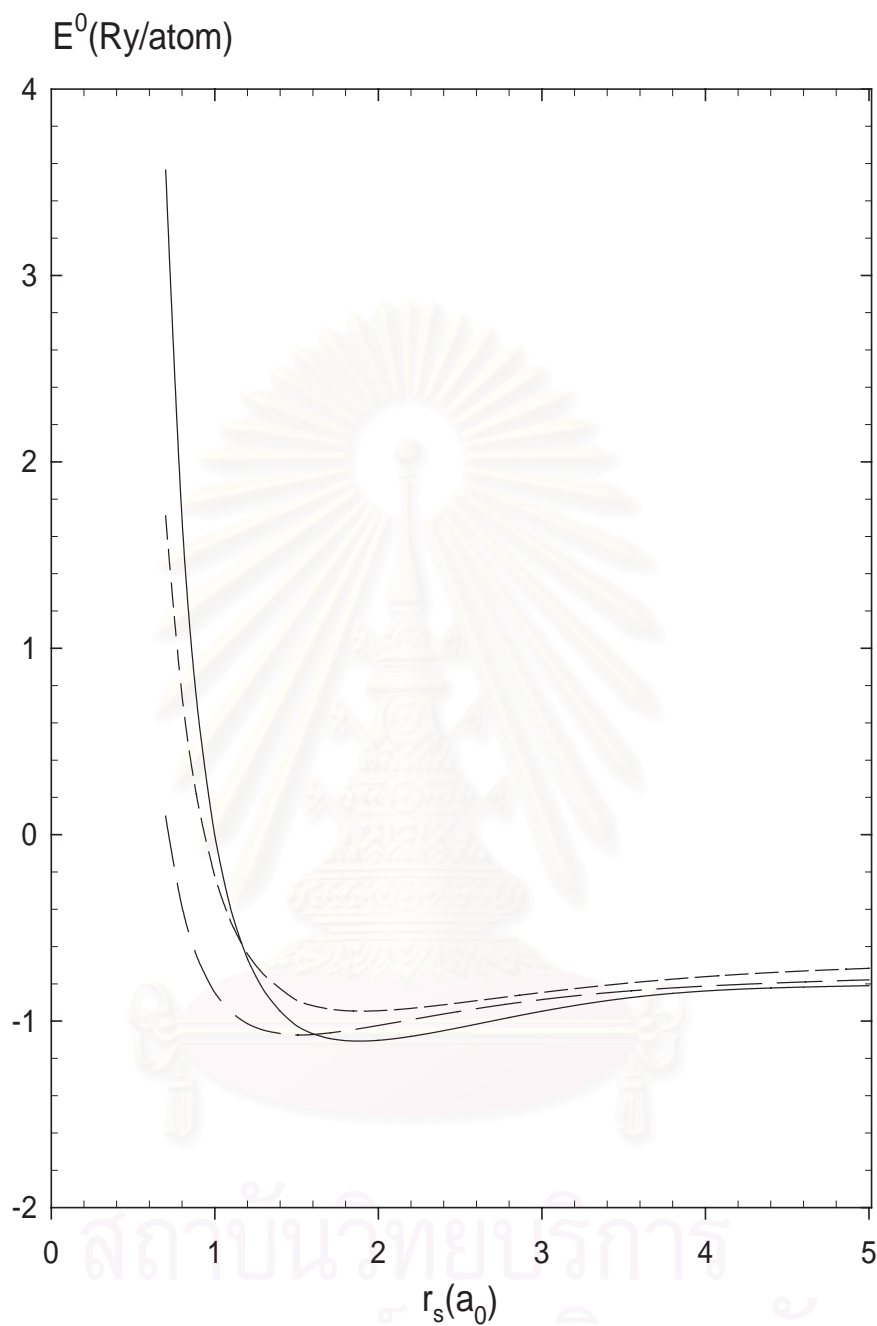


Fig.5.1. Ground state energy calculated by the Wigner-Seitz method with various potentials: Coulomb potential (solid line), the uniform screened Coulomb potential (long dashed line) and the Thomas-Fermi screened potential (short dashed

line).

Following the estimation of the other terms in Eq. (3.31) proposed by Styer and Ashcroft[7], the ground state energy as a function of r_s is shown in Fig.5.1. For Coulomb potential(solid line), the minimum energy is -1.10 Ry/atom at $r_s=1.8a_0$ which corresponds to a density of 0.44 g/cm^3 . For uniform screening (long dashed line), the minimum energy is -1.07Ry/atom at $r_s=1.6a_0$. For Thomas-Fermi screening (short dashed line), the minimum energy is -0.94Ry/atom at $r_s=1.8a_0$. For comparison, the minimum ground state energy calculated by Styer and Ashcroft[7] is -1.078Ry/atom at $r_s=1.66a_0$, -1.038 Ry/atom at $r_s=1.65a_0$ and -1.052 Ry/atom at $r_s=1.61a_0$ for Coulomb, the uniform screened and Thomas-Fermi screened potential Coulomb potentials, respectively.

5.3 The Ground State Properties of the Solid Metallic Hydrogen by the Full Potential Linearized Augmented Plane Wave Method

In this section, we represent the results of our calculations, i.e. the energy band structure, the density of states and the ground state energy of solid metallic hydrogen in some different atomic structures. The ground state energy is calculated by using Eq. (4.95) and the density of states is evaluated by using the tetrahedron method, described in section 4.4.4.

5.3.1 The Energy Band Structure

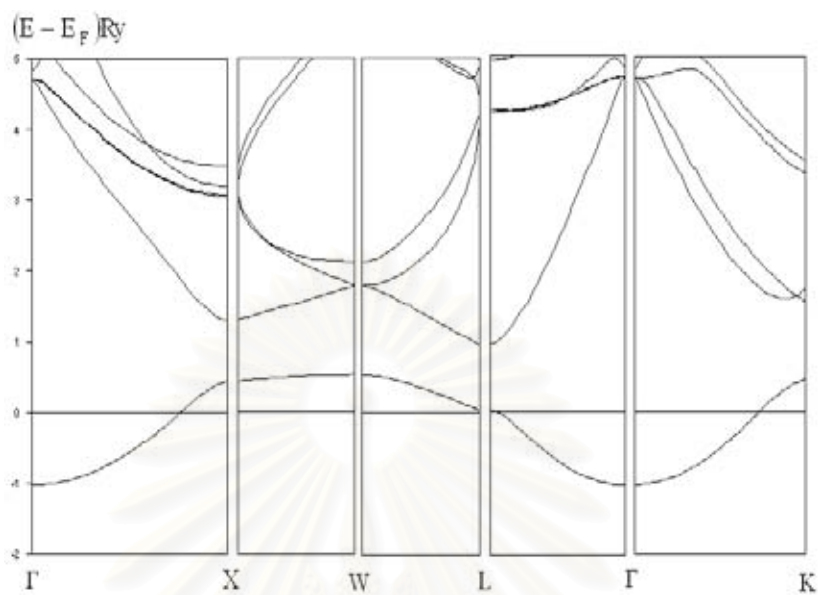


Fig. 5.2 The energy band structure of the solid metallic hydrogen in a face-centered cubic structure.

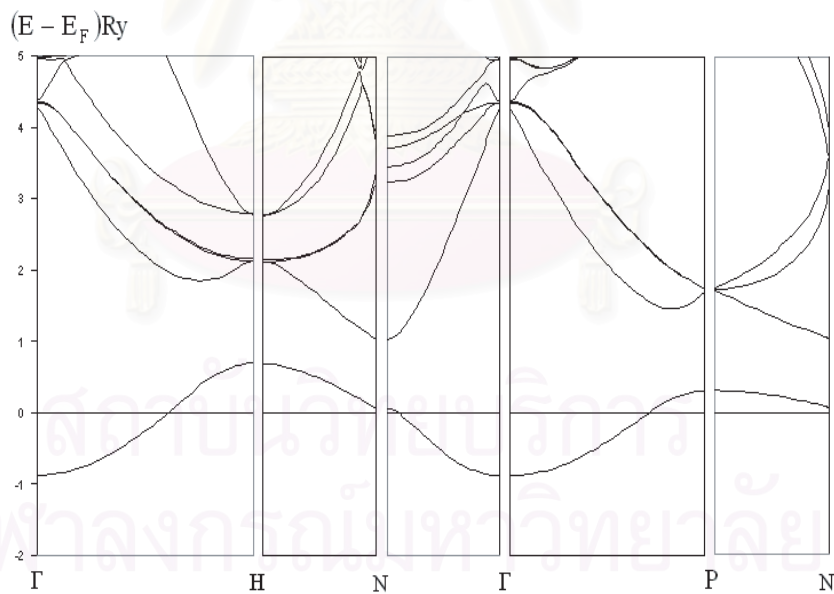


Fig. 5.3 The energy band structure of the solid metallic hydrogen in a body-centered cubic structure.

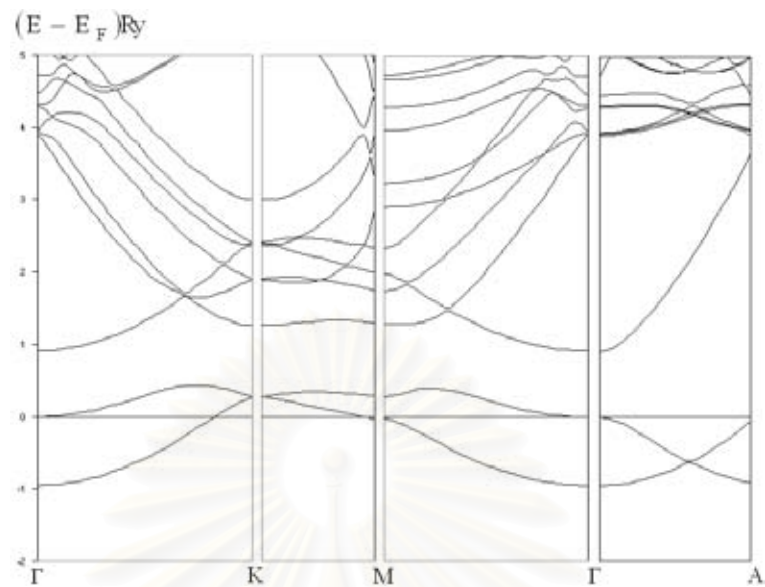


Fig. 5.4 The energy band structure of the solid metallic hydrogen in a hexagonal close-packed structure.

5.3.2 The Density of States

By using the tetrahedron method, the density of states is calculated by using Eq. (4.47-4.55).

สถาบันวิทยบริการ
จุฬาลงกรณ์มหาวิทยาลัย

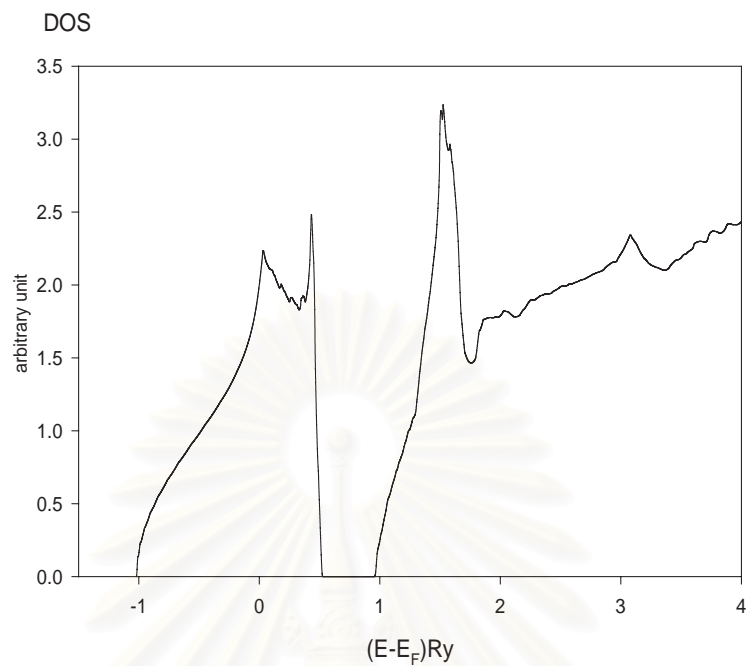


Fig. 5.5 The density of states of the solid metallic hydrogen in a face-centered cubic structure.

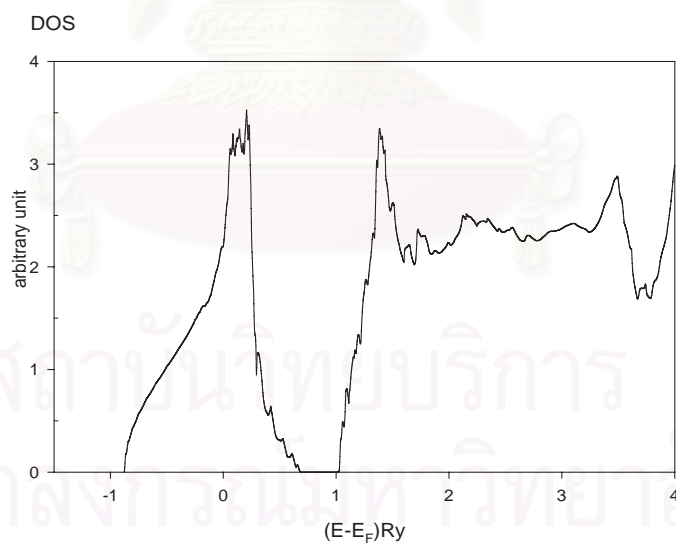


Fig. 5.6 The density of states of the solid metallic hydrogen in a body-centered cubic structure.

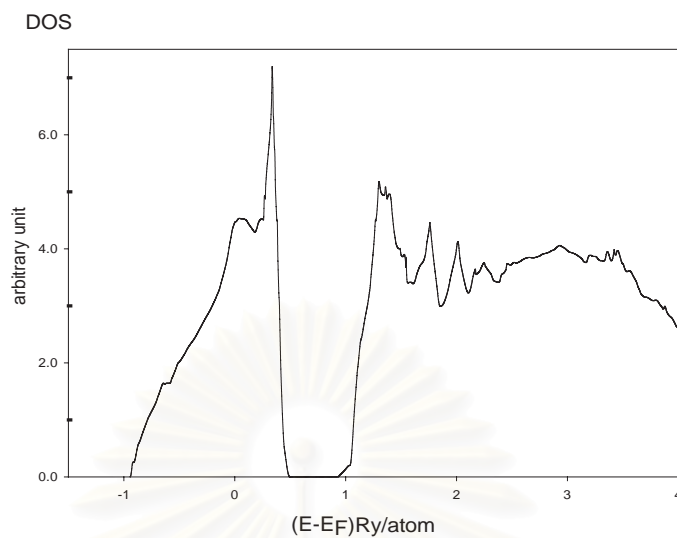


Fig. 5.7 The density of states of the solid metallic hydrogen in a hexagonal close-packed structure.

The density of states of the solid hydrogen in three structures show the Fermi energy in the conduction band which mean that the solid hydrogen is a metal.

5.3.3 The total Ground State Energy

From the total energy calculation, we calculate the total ground state energy of metallic hydrogen as function of r_s by using Eq.(4.95).

สถาบันวิทยบริการ
จุฬาลงกรณ์มหาวิทยาลัย

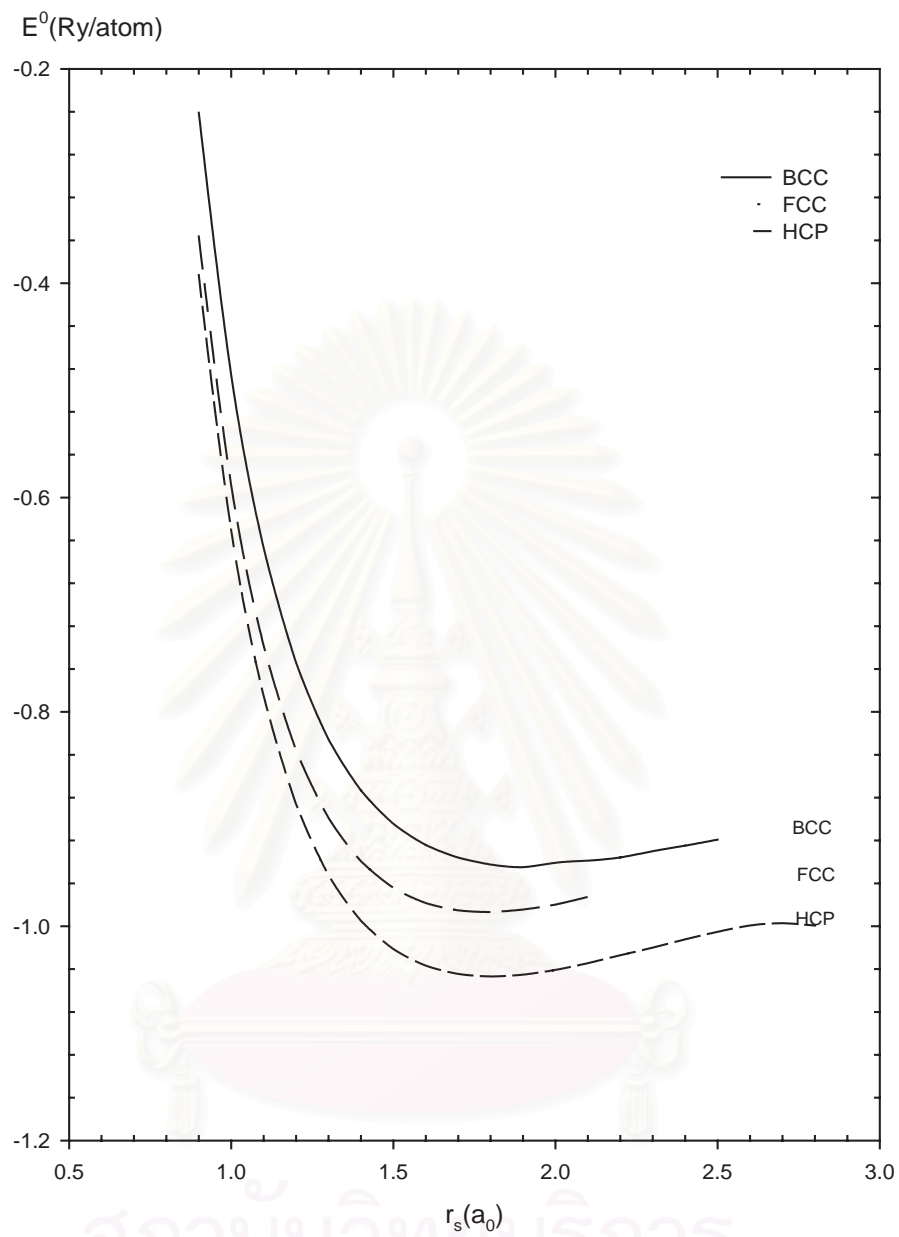


Fig. 5.8 The total ground state energy of metallic hydrogen with various atomic structures: a face-centered cubic(long dashed line), a body-centered cubic(solid line) and a hexagonal close-packed(short dashed line)

For the face-centered cubic structure (solid line), the minimum energy is about -0.98 Ry/atom at $r_s=1.75a_0$. For the body-centered cubic structure (short dashed line), the minimum energy is about -0.94 Ry/atom at $r_s=1.85a_0$. For the hexagonal close-packed structure (long dashed line), the minimum energy is -1.05 Ry/atom at $1.80a_0$.

5.4 Discussion

In the calculations of the ground state energy of the solid metallic hydrogen by the Wigner-Seitz method which based on the Hartree-Fock theory, our results show effects of the screening interaction between the electrons and their own nuclei, and the interaction among the nuclei. In Styer and Ashcroft 's work[7], the screening effects have no obvious impact on the physical properties of the metallic hydrogen. This is contrast with our findings. We see that the minimum ground state energy is higher in the case of Thomas-Fermi screened Coulomb potential than in the case of Coulomb potential. In the uniform screening, the volume is small because the interaction caused by the uniform screened potential has a very short range effect, *i.e.* $U(r)$ vanishes at the cell boundary. Thus the nuclei can hardly see each other and tend to stay closer together.

However, the total ground state energy of the metallic hydrogen does not depend on the structure. In addition, a nearly free electron wave is used in the calculation of the exchange energy and the Hartree energy. To improve

our calculations, we choose the full potential linearized augmented plane wave based on the density functional theory to solve this problem. The results of this method in different structures show that the total ground state energy is minimum in the hexagonal close-packed. This agrees well with other works[36] which is the calculation of the ground state of solid molecular hydrogen in various structures. The density of states below the Fermi level calculated in the full potential linearized augmented plane wave method is similar to the density of states calculated in the Wigner-Seitz method up to the Fermi level. It implies that the Wigner-Seitz method is applicable.



สถาบันวิทยบริการ
จุฬาลงกรณ์มหาวิทยาลัย

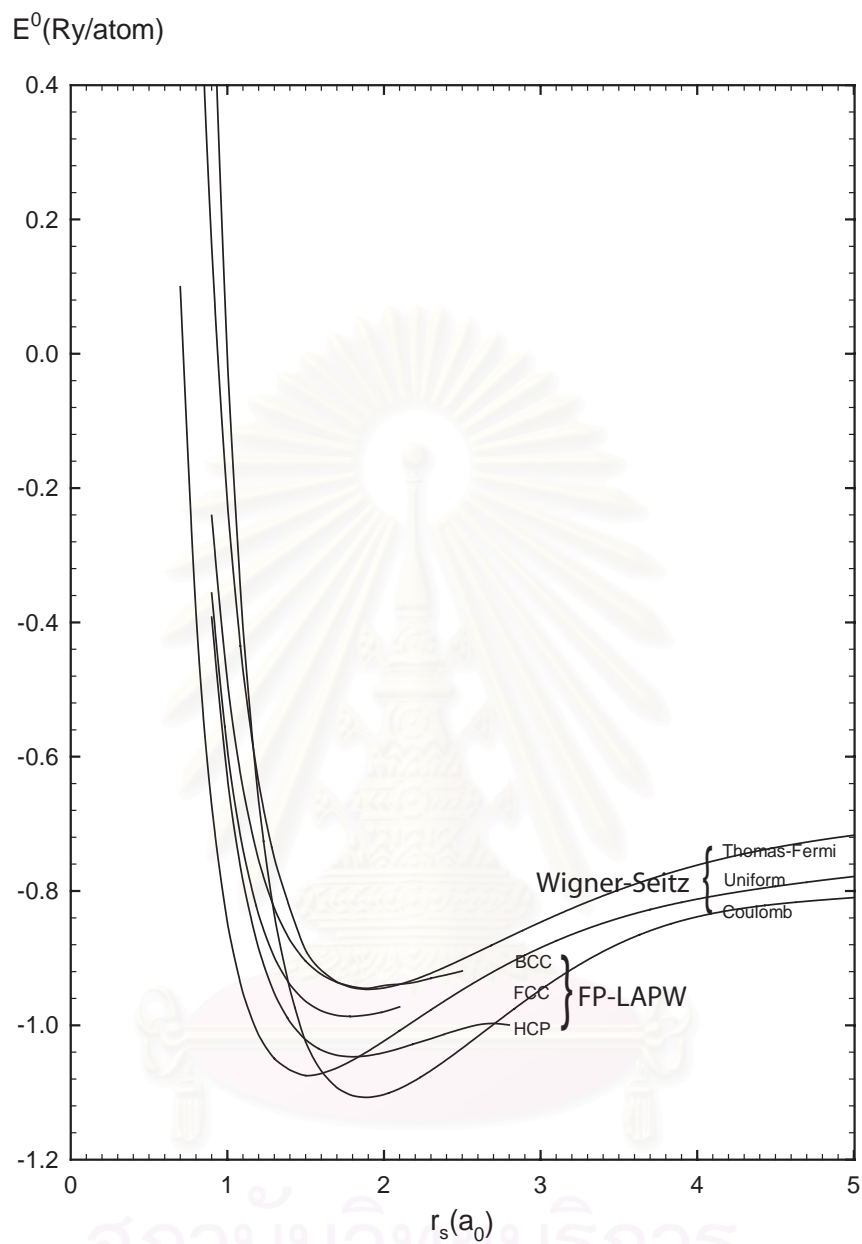


Fig. 5.9 A comparison of the total ground state energy of the metallic hydrogen between Wigner-Seitz method and the full potential linearized augmented plane wave.

However, this calculation method is based on the local density functional

approximation which is used in a homogeneous electron system. In future work, we will use a generalized gradient approximation or an exact exchange in the density functional theory. In addition, we will include the contribution of ionic motions at finite temperatures.



สถาบันวิทยบริการ
จุฬาลงกรณ์มหาวิทยาลัย

Chapter 6

Conclusions

In the present work, we investigate the total ground-state energy of solid metallic hydrogen as a function of r_s and to determine r_s at which the ground state energy is minimum. We assume that the solid metallic hydrogen consists of electrons and protons which occupy the sites of a rigid Bravais lattice. The many-body problem is solved by using the Hartree-Fock theory and the density functional theory. The total ground state energy is calculated by using the Wigner-Seitz method and the full potential linearized augmented plane wave. We use the Wigner-Seitz method to estimate the energy band dispersion upto $o(k^4)$ and use the most accurate correlation potential available. Under the simple Coulomb potential, the minimum ground state energy is 1.10 Ry/atom at $r_s=1.8 a_0$ which corresponds to the density of $0.44 g/cm^3$. Under screening by the uniform screening and Thomas-Fermi screening, the minimum ground state energy are -1.07 Ry/atom at $r_s=1.6a_0$ and -0.94 Ry/atom at $r_s=1.8a_0$ respectively. Normal metals have r_s between $2.0a_0 - 6.0a_0$. The density of lithium is $0.542 g/cm^3$ and the density of

iron is 7.87 g/cm^3 .

To improve our works, we also apply the FP-LAPW method. In the full potential linearized augmented plane wave, we calculate the total ground state energy, the density of states and the band energy structure in various atomic structures. In the body-centered cubic and the face-centered cubic structures, the solid hydrogen is a metal with the minimum ground state energy about -0.94Ry/atom and -0.98Ry/atom at $r_s=1.85a_0$ and $r_s=1.75a_0$ respectively. In the hexagonal close-packed, the solid hydrogen is a metal with the ground state energy about -1.05Ry/atom at $r_s=1.8a_0$. Our results agree with other's results in that the hexagonal close-packed structure has the lower ground state energy than the face-centered cubic and the body-centered cubic structures[35]. When we consider the density of states, we find that the density of states below Fermi energy calculated by the full potential linearized augmented plane wave has a similar as the density of states approximated by the Wigner-Seitz method. It implies that the Wigner-Seitz method is simple and yet applicable approximation for alkali metals.

From our calculations, they confirm that there is possibility that the solid metallic hydrogen exists because the ground state energy is negative. However, the determination of the phase transition point is very difficult. According to experiments, hydrogen does not become a metallic solid under the highest pressure

available in laboratory, i.e. about 340 GPa[36]. Furthermore, solid molecular hydrogen[7] has lower ground state energy which is -1.1648 Ry/atom at $r_s = 3.12a_0$. Thus it is more likely that the solid molecular hydrogen will be found under pressure instead of the solid metallic hydrogen because the nature will be in its lowest energy state. The solid metallic hydrogen might exist as a metastable state. If it is stable, there must be some other effects, apart from those effects included in this work, which reduce the total ground state energy. Recently there has been a report on collective excitations, which produce extra binding energy and might cause the metallization. However, this is beyond the scope of the present work.



References

- [1] E. Wigner and H.B. Huntington. On the possibility of a metallic modification of hydrogen. J. Chem. Phys 3(1935) : 764.
- [2] E. G. Maksomov and D. Y. Savrasov and H.B. Huntington. Lattice stability and superconductivity of the metallic hydrogen at high pressure. Solid State Comm. 119(2001) : 569.
- [3] W. J. Nellis. Metallization of hydrogen and other small molecules at 100 GPa pressure. High Pressure Research 22 (2002) : 655.
- [4] S. Raimes. The Wave Mechanics of Electrons in Metals. Amsterdam : North-Holland Publishing Company, 1970.
- [5] J. M. Thijssen. Computational Physics. London : Cambridge University Press, 1999.
- [6] R. G. Parr and W. Yang. Density-Functional Theory of Atoms and Molecules. New York : Oxford University Press, 1989.
- [7] D. F. Styer and N. W. Aschroft. Ground-state energy of metallic hydrogen in the Wigner-Seitz approximation. Phys. Rev. B 29 (1984) : 5562.
- [8] S. Massidda, M. Posternak, and A. Baldereschi. Hartree-Fock LAPW approach to the electronic properties of periodic system. Phys. Rev. B 48(1993) : 5058.
- [9] W. Kohn and L. J. Sham . Self-consistent equations including exchange and correlation effects. Phys. Rev. 140(1965) : 1133.
- [10] C. Kittel. Introduction to Solid State Physics 7th ed.. New York : John Wiley and Sons, 1996.
- [11] J. Callaway. Energy Band Theory. New York : Academic Press, 1964.
- [12] J. Bardeen . An improved calculation of the energies of metallic Li and Na. J. Chem. Phys. 6(1938) : 367.
- [13] R. A. Silverman . Fermi energy of metallic lithium. Phys. Rev. 85 (1952) : 227.
- [14] G. B. Arfken and H. J. Weber. Mathematical Methods for Physicists. New York : Academic Press, 1995.
- [15] O. Madelung. Introduction to Solid-State Theory. New York : Springer Verlag, 1978.

- [16] S. H. Vosko, L. Wilk and M. Nusair. Fermi energy of metallic lithium. Can. J. Phys 58(1980) : 1200.
- [17] R. L. Liboff. Quantum Mechanics 3rd ed.. New York : Addison-Wesley, 1997.
- [18] E. C. Snow And J. T. Waber. Self-consistent energy band of metallic copper by the augmented plane wave method. Phys. Rev. 157 (1962) : 570.
- [19] T. L. Loucks. Augmented Plane Wave Method. New York : W. A. Benjamin, 1967.
- [20] M. Weinert, E. Wimmer and A. J. Freeman. Total-energy all-electron density functional method for bulk solids and surfaces. Phys. Rev. B. 26(1982) : 4571.
- [21] David Singh. Ground-state properties of lanthanum: treatment of extended-core state. Phys. Rev. B. 43(1991) : 6388.
- [22] N. A. W. Holzwarth, G. E. Matthews and Y. Zeng. Comparison of the projector augmented plane wave, pseudopotential and linearized augmented plane wave formalisms for density functional calculations of solids. Phys. Rev. B. 55(1997) : 2005.
- [23] D. D. Koelling and G. O. Arbman. Use of the energy derivative of the radial solution in an augmented plane wave method: application to copper. J. Phys. F. 5(1975) : 2041.
- [24] O. K. Andersen. Linear method in band theory. Phys. Rev. B. 12 (1975) : 3060.
- [25] P. E. Blochl. Improved tetrahedron method for Brillouin zone integrations. Phys. Rev. B. 49(1994) : 16223.
- [26] O. Jepsen and O. K. Andersen. No error in the tetrahedron integration scheme. Phys. Rev. B. 29(1984) : 5965.
- [27] D. J. Chadi and Marvin L. Cohen. Special points in the Brillouin zone. Phys. Rev. B. 8(1973) : 5747.
- [28] Hendrik J. Monkhorst and James D. Pack. Special points for Brillouin integrations. Phys. Rev. B. 13(1976) : 5188.
- [29] A. Baldereschi. Mean value point in the Brillouin zone. Phys. Rev. B. 7(1973) : 5215.
- [30] Max Petersen, Frank Wagner and Karlheinz Schwarz. Improving the efficiency of FP-LAPW calculations. Comp. Phys. Commun. 126(2000) : 294.
- [31] A. B. Shick, A. I. Liechtenstein. Implementation of the LDA+U method using the full potential linearized augmented plane wave basis. Phys. Rev. B. 60(1999) : 10763.

- [32] C. P. Beulshausen and L. Fritsche. Viable improvement of the full potential linearized augmented plane wave (FLAPW) method. Eur. Phys. J. B. 2(1998) : 237.
- [33] Philipp Kurz. Non Collinear Magnetism of Ultrathin Magnetic Films. Diplomarbeit Physik Mathematisch-Naturwissenschaftlichen Institut für Festkörperforschung Forschungszentrum Jülich, 1997.
- [34] M. Weinert. Solution of poisson's equation: beyond Ewald-type methods . J. Math. Phys 22(1981) : 2433.
- [35] M. Stadel and R. M. Martin. Metallization of molecular hydrogen. Preprint, con-mat:0003035. (Mar 2000).
- [36] C. Narayana, H. Luo, J. Orloff and A. L. Ruoff. Solid hydrogen at 342 GPa: no evidence for an alkali metal . Nature 393(1998) : 46.
- [37] P. Moontragoon and U. Pinsook. Metallic hydrogen in a more accurate Wigner-Seitz approximation . J. Sci. Res. Chula Univ. 28(2003) : 14.



สถาบันวิทยบริการ
จุฬาลงกรณ์มหาวิทยาลัย

Biography

Mr.Pairot Moontragoon was born on September 28,1977 in Srisaket. He received B. Sc. degree (second class honor) in physics from Khonkaen University in 1999.



สถาบันวิทยบริการ
จุฬาลงกรณ์มหาวิทยาลัย